established. Here, the safety of intraventricular PPS infusion at up to a dose yielding the maximal effectiveness in mice was demonstrated in experimental animals. However, at higher doses than this, there was a gap between small rodents and dogs, with the dogs showing adverse effects, such as seizures that were mostly caused by hematoma formation around the intraventricular cannula, although such adverse effects appeared only very early in the treatment. It is well known that smaller animals metabolize drugs much more quickly, and therefore intraventricular PPS at the same dosage was not toxic in mice and rats but was toxic in dogs. For application of this treatment to humans, it will be important to take account of the drug metabolism differences between mice and humans.

Amphotericin B and one of its derivatives are known to prolong the life spans of infected animals even with administration late in the disease course (8). In our experiments, however, amphotericin B did not cause any significant prolongation at a late-stage administration. Differences in the administration route, dose, and duration, as well as the experimental models, might account for this difference, but it remains to be elucidated.

Antimalarial chemicals, including quinacrine, had no effects in the present studies. These chemicals were previously found to be effective in inhibiting abnormal PrP formation in a scrapie-infected cell line (10, 15), and quinacrine has been used in clinical trials for TSE patients. However, together with the recent findings of two other research groups (1, 6), our data suggest that quinacrine may not improve the prognosis of the patients.

Finally, the placement of an intraventricular cannula in TSE patients may create public health issues due to fears of contamination of the operating room or safety issues with respect to the personnel involved with this procedure. For these reasons, other drug delivery systems which do not need a surgical procedure should be developed, and PPS derivatives that can be delivered into the brain after peripheral administration also need to be developed. As an immediately applicable remedy, however, continuous intraventricular PPS administration with an infusion device may be a candidate for a clinical trial, with a view to preventing the disease in those people categorized as being at extremely high risk or to improving the prognosis of diseased people with TSEs.

ACKNOWLEDGMENTS

This study was supported by grants to K.D. from the Ministry of Health, Labour and Welfare (H13-kokoro-025) and from the Ministry of Education, Culture, Sports, Science and Technology (13557118 and 14021085), Tokyo, Japan.

We thank B. Chesebro of the Rocky Mountain Laboratories, National Institute of Allergy and Infectious Diseases, National Institutes of Health, for providing the Tg7 mice and C. Weissmann of the Imperial College School of Medicine at St. Mary's, London, United Kingdom, for providing the Tga20 mice. We also thank I. Goto for the electroencephalogram analyses.

REFERENCES

1. **Barret, A., F. Tagliavini, G. Forloni, C. Bate, M. Salmona, L. Colombo, A. De Luigi, L. Limido, S. Suardi, G. Rossi, F. Auvré, K. T. Adjou, N. Salés, A. Williams, C. Lasmézas, and J. P. Deslys.** 2003. Evaluation of quinacrine treatment for prion diseases. J. Virol. 77:8462–8469.
2. **Brown, P.** 2002. Drug therapy in human and experimental transmissible spongiform encephalopathy. Neurology 58:1720–1725.
3. **Brown, P., M. Preece, J. P. Brandel, T. Sato, L. McShane, I. Zerr, A. Fletcher, R. G. Will, M. Pocchiari, N. R. Cashman, J. H. d'Aignaux, L. Cervenakova, J. Fradkin, L. B. Schonberger, and S. J. Collins.** 2000. Iatrogenic Creutzfeldt-Jakob disease at the millennium. Neurology 55:1075–1081.
4. **Caughey, B., K. Brown, G. J. Raymond, G. E. Katzenstein, and W. Thresher.** 1994. Binding of the protease-sensitive form of PrP (prion protein) to sulfated glycosaminoglycan and Congo red. J. Virol. 68:2135–2141.
5. **Caughey, B., and G. J. Raymond.** 1993. Sulfated polyanion inhibition of scrapie-associated PrP accumulation in cultured cells. J. Virol. 67:643–650.
6. **Collins, S. J., V. Lewis, M. Brazier, A. F. Hill, A. Fletcher, and C. L. Masters.** 2002. Quinacrine does not prolong survival in a murine Creutzfeldt-Jakob disease model. Ann. Neurol. 52:503–506.
7. **Dealler, S.** 1998. Post-exposure prophylaxis after accidental prion inoculation. Lancet 351:600.
8. **Demaimay, R., K. T. Adjou, V. Beringue, S. Demart, C. I. Lasmézas, J. P. Deslys, M. Seman, and D. Dormont.** 1997. Late treatment with polyene antibiotics can prolong the survival time of scrapie-infected animals. J. Virol. 71:9685–9689.
9. **Diringer, H., and B. Ehlers.** 1991. Chemoprophylaxis of scrapie in mice. J. Gen. Virol. 72:457–460.
10. **Doh-ura, K., T. Iwaki, and B. Caughey.** 2000. Lysosomotropic agents and cysteine protease inhibitors inhibit scrapie-associated prion protein accumulation. J. Virol. 74:4894–4897.
11. **Doh-ura, K., E. Mekada, K. Ogomori, and T. Iwaki.** 2000. Enhanced CD9 expression in the mouse and human brains infected with transmissible spongiform encephalopathies. J. Neuropathol. Exp. Neurol. 59:774–785.
12. **Ehlers, B., and H. Diringer.** 1984. Dextran sulphate 500 delays and prevents mouse scrapie by impairment of agent replication in spleen. J. Gen. Virol. 65:1325–1330.
13. **Farquhar, C., A. Dickinson, and M. Bruce.** 1999. Prophylactic potential of pentosan polysulphate in transmissible spongiform encephalopathies. Lancet 353:117.
14. **Fischer, M., T. Rulicke, A. Raeber, A. Sailer, M. Moser, B. Oesch, S. Brandner, A. Aguzzi, and C. Weissmann.** 1996. Prion protein (PrP) with amino-proximal deletions restoring susceptibility of PrP knockout mice to scrapie. EMBO J. 15:1255–1264.
15. **Korth, C., B. C. May, F. E. Cohen, and S. B. Prusiner.** 2001. Acridine and phenothiazine derivatives as pharmacotherapeutics for prion disease. Proc. Natl. Acad. Sci. USA 98:9836–9841.
16. **Ladogana, A., P. Casaccia, L. Ingrosso, M. Cibati, M. Salvatore, Y. G. Xi, C. Masullo, and M. Pocchiari.** 1992. Sulphate polyanions prolong the incubation period of scrapie-infected hamsters. J. Gen. Virol. 73:661–665.
17. **Priola, S. A., B. Caughey, and W. S. Caughey.** 1999. Novel therapeutic uses for porphyrins and phthalocyanines in the transmissible spongiform encephalopathies. Curr. Opin. Microbiol. 2:563–566.
18. **Prusiner, S. B.** 1998. Prions. Proc. Natl. Acad. Sci. USA 95:13363–13383.
19. **Race, R. E., S. A. Priola, R. A. Bessen, D. Ernst, J. Dockter, G. F. Rall, L. Mucke, B. Chesebro, and M. B. Oldstone.** 1995. Neuron-specific expression of a hamster prion protein minigene in transgenic mice induces susceptibility to hamster scrapie agent. Neuron 15:1183–1191.
20. **Shyng, S. L., S. Lehmann, K. L. Moulder, and D. A. Harris.** 1995. Sulfated glycans stimulate endocytosis of the cellular isoform of the prion protein, PrPC, in cultured cells. J. Biol. Chem. 270:30221–30229.
21. **Will, R. G., J. W. Ironside, M. Zeidler, S. N. Cousens, K. Estibeiro, A. Alperovitch, S. Poser, M. Pocchiari, A. Hofman, and P. G. Smith.** 1996. A new variant of Creutzfeldt-Jakob disease in the UK. Lancet 347:921–925.
22. **Wong, C., L. W. Xiong, M. Horiuchi, L. Raymond, K. Wehrly, B. Chesebro, and B. Caughey.** 2001. Sulfated glycans and elevated temperature stimulate PrP(Sc)-dependent cell-free formation of protease-resistant prion protein. EMBO J. 20:377–386.

Laboratory Investigation (2004) 84, 828–835

www.laboratoryinvestigation.org

Accumulation of prion protein in muscle fibers of experimental chloroquine myopathy: *in vivo* model for deposition of prion protein in non-neuronal tissues

Hisako Furukawa*, Katsumi Doh-ura†, Kensuke Sasaki and Toru Iwaki

Department of Neuropathology, Neurological Institute, Graduate School of Medical Sciences, Kyushu University, Fukuoka, Japan

Prion protein (PrP) is known to accumulate in some non-neuronal tissues under conditions unrelated to prion diseases. The biochemical and biological nature of such accumulated PrP molecules, however, has not been fully evaluated. In this study, we established experimental myopathy in hamsters by long-term administration of chloroquine, and we examined the nature of the PrP molecules that accumulated. PrP accumulation was immunohistochemically demonstrated in autophagic vacuoles in degenerated muscle fibers, and this was accompanied by the accumulation of other molecules related to the neuropathogenesis of prion diseases such as clathrin, cathepsin B, heparan sulfate, and apolipoprotein J. Accumulated PrP molecules were partially insoluble in detergent solution and were slightly less sensitive to proteinase K digestion than normal cellular PrP. Muscle homogenates containing these PrP molecules did not cause disease in inoculated hamsters. The findings indicate that the PrP molecules that accumulated in muscle fibers have distinct biochemical and biological properties. Therefore, experimental chloroquine myopathy is a novel and useful model to investigate the mechanism of deposition of PrP in non-neuronal tissues and might provide new insights in the pathogenesis of prion diseases.
Laboratory Investigation (2004) **84**, 828–835, advance online publication, 3 May 2004; doi:10.1038/labinvest.3700111

Keywords: detergent-solubility; experimental chloroquine myopathy; lysosome; non-neuronal tissues; prion protein; protease sensitivity

Prion diseases such as Creutzfeldt–Jakob disease in humans, and scrapie and bovine spongiform encephalopathy in animals are neurodegenerative disorders characterized by the accumulation in the brain of a protease-resistant, detergent-insoluble abnormal isoform of prion protein (PrP). This abnormal isoform of PrP (PrP^{Sc}) is pathogenic itself and replicates by altering the conformation of a protease-sensitive, detergent-soluble normal cellular isoform of prion protein (PrP^{C}).[1] In addition to the central nervous system, PrP^{Sc} deposition is observed in non-neuronal tissue such as tonsils and skeletal muscles in human prion diseases[2,3] and experimental animals.[4]

PrP is also known to accumulate in non-neuronal tissues under certain pathological conditions unrelated to prion diseases. Frederiske *et al*[5] recently revealed increased PrP immunoreactivity in the regions of fiber-cell degeneration in cataractous lenses in humans. Askanas *et al*[6] reported the accumulation of PrP in vacuolated muscle fibers, in angulated and round atrophic fibers with sarcolemmal enhancement, and in the perivascular inflammatory cells of sporadic inclusion-body myositis in humans.[6,7] It was also reported that the accumulated PrP molecules were sensitive to protease treatment.[7] However, the biochemical and biological characteristics of these PrP molecules have not been fully evaluated.

Chloroquine, a widely used antimalarial agent, is known to be concentrated in lysosomes and to cause elevation of intralysosomal pH.[8] Long-term

Correspondence: Dr H Furukawa, MD, PhD, Department of Pharmacology 1, Nagasaki University Graduate School of Biomedical Sciences, 1-12-4 Sakamoto, Nagasaki 852-8523, Japan.
E-mail: hisako@net.nagasaki-u.ac.jp
*Current address: Department of Pharmacology 1, Nagasaki University Graduate School of Biomedical Sciences, 1-12-4 Sakamoto, Nagasaki 852-8523, Japan.
†Division of Prion Protein Biology, Department of Prion Research, Tohoku University Graduate School of Medicine, 2-1 Seiryo-cho, Aoba-ku, Sendai 980-8575, Japan.
Received 16 January 2004; revised 7 March 2004; accepted 12 March 2004; published online 3 May 2004

administration of chloroquine sometimes causes myopathy, termed chloroquine myopathy (CM), which is characterized by degenerated muscle fibers with numerous autophagic, rimmed vacuoles.[9] Tsuzuki *et al*[10] established experimental CM in the rat to investigate the mechanism of accumulation of the proteins related to Alzheimer's disease in rimmed vacuoles, because of its histopathological similarity to human myopathies where amyloid β deposition is observed in rimmed vacuoles.

To explore the biochemical and biological properties of PrP molecules that accumulate under pathological conditions unrelated to prion diseases, we established experimental CM in hamsters and characterized the PrP molecules (PrP^{CQ}) that accumulated in affected muscle fibers.

Materials and methods

Animals and Reagents

Female Syrian hamsters, 3–8-week old, were purchased from SLC (Hamamatsu, Japan). Chloroquine diphosphate and Nonidet P-40 (NP-40) were purchased from Sigma Chemical (MO, USA). Proteinase K (PK) and complete mini protease inhibitor cocktail were obtained from Roche Molecular Biochemicals (Germany). Monoclonal antibody 3F4 recognizing hamster PrP109-112 was from Senetek (St Louis, MO, USA). Anti-prion protein polyclonal antibody PrP2B was raised by immunization of rabbits with a hamster PrP89-103 fragment. Polyclonal antibodies for apolipoprotein J (clusterin) and for cathepsin B, and monoclonal antibodies CHC5.9 for clathrin and HepSS-1 for heparan sulfate were purchased from Chemicon (Temecula, CA, USA), Calbiochem (Cambridge, MA, USA), PROGEN Biotechnik GmbH (Germany), and Seikagaku Corporation (Japan), respectively.

Experimental CM in Hamsters

Hamsters received 50 mg/kg chloroquine diphosphate (10 mg/ml in sterile saline, pH 7.6) as daily intraperitoneal injections for 60 days. Then the hamsters were killed by decapitation under deep anesthesia. Bilateral soleus, tibialis anterior, and quadriceps muscles were removed and immediately snap-frozen in isopentane cooled with liquid nitrogen. Frozen muscles were kept at −80°C until analysis.

Immunohistochemical Studies

After the blockage of endogenous peroxidase with 0.3% hydrogen peroxide in methanol, serial 10-μm thick sections of frozen muscle were incubated overnight at 4°C with the primary antibodies diluted with 10 mM phosphate-buffered saline (PBS) containing 1% normal hamster serum. The sections were then incubated with horseradish peroxidase-conjugated secondary antibodies for 1 h followed by reactions with 3,3′-diaminobenzidine/H_2O_2 and counterstained with hematoxylin. The serial sections were stained with hematoxylin and eosin (HE), or stained for acid phosphatase or by a modified Gomori-trichrome method.

Brain specimens obtained in some experiments were immersion-fixed in 10% buffered formalin for 24 h at 4°C and embedded in paraffin for immunohistochemical examination. For detection of abnormal PrP deposition, deparaffinized 8-μm thick sections were treated with hydrolytic autoclaving prior to incubation with 3F4 monoclonal antibody.[11]

Protease Sensitivity Assay of PrP^{CQ}

After confirmation of the histological findings, the remaining frozen muscle was homogenized using Tissue-Tearor (Biospec Products, Oklahoma) in 10 volumes of lysis buffer A (0.5% NP-40, 0.5% sodium deoxycholate in PBS pH 7.4). Homogenates were centrifuged at $3300 \times g$ for 15 min to remove the nuclear fraction and debris. The supernatant was then treated with the indicated amount of PK at 37°C for 20 min. After stopping the digestion with 4 mM 4-[2-aminoethyl]-benzenesulfonyl fluoride (Pefabloc, Roche, Germany), an aliquot corresponding to 4 mg of muscle tissue was analyzed by Western blotting using polyclonal antibody PrP2B. Labeled PrP was visualized by using CDP-star detection reagent (Amersham, UK).

Detergent Solubility Assay of PrP^{CQ}

The detergent solubility of PrP^{CQ} was determined as described by Lehmann and Harris[12] with minor modification. Briefly, soleus muscle samples from either control or CM hamsters were homogenized in lysis buffer B (15 mM NaCl, 50 mM Tris-HCl pH 7.5, complete-mini protease inhibitor cocktail) containing the designated concentration of NP-40. Homogenate was centrifuged for 5 min at 1600 *g* to remove debris and the nuclear fraction. The supernatant was ultracentrifuged at 265 000 *g* for 40 min at 25°C. Proteins in the supernatant and in the pellet were separately recovered and analyzed by Western blotting using monoclonal antibody 3F4.

Intracerebral Inoculation of PrP^{CQ}

Inoculum was prepared by homogenizing muscular tissue from CM hamsters or the control in 10 volumes of sterile saline, and 20 μl of the inoculum was injected into the brain of 19 3-week-old female hamsters under deep anesthesia. The hamsters were observed for over 2 years and killed to examine PrP molecules in the brain immunohistochemically.

Densitometry and Statistical Analysis

Blots of the gels were scanned with a CanoScan D2400UF (Canon, Japan). Densities of bands were quantified using NIH Image software. Statistical significance of densitometric data was analyzed by repeated measure ANOVA, and statistical comparison at each dose point between groups was made by Student's *t*-test or Welch's *t*-test.

Ethics

Animal handling and killing were in accordance with the nationally prescribed guidelines, with ethical approval for the study granted by the Animal Experiment Committee of Kyushu University.

Results

Histochemical Findings of CM

All the muscle specimens taken from chloroquine-treated hamsters showed various degrees of myopathic changes accompanied with rimmed vacuoles (Figure 1a), and this was consistent with histopathological findings of experimental CM in the rat.[9,10] In addition to the rimmed vacuoles, many muscle fibers contained coarse granular structures that were strongly stained by hematoxylin (Figure 1c) and modified Gomori trichrome stain (Figure 1g), and they showed enhanced acid phosphatase activity (Figure 1h). These abnormal structures were observed in about 10% of muscle fibers in the soleus muscle which was the most affected in all the muscles of chloroquine-treated hamsters. In contrast, muscles of control hamsters did not contain any rimmed vacuoles or coarse granular structures.

All of the rimmed vacuoles and the coarsely granular structures in degenerated muscle fibers of CM were positively stained by an anti-PrP monoclonal antibody, 3F4, recognizing hamster PrP109-112 (Figure 1b, d). In control hamster muscles, the 3F4 monoclonal antibody reacted with sarcolemmal membranes (data not shown).

To investigate the possible involvement of some molecules that relate to the metabolism of PrP^{C} or the deposition of PrP^{Sc}, serial sections were immunostained for apolipoprotein J (Figure 1e), clathrin (Figure 1f), cathepsin B (Figure 1i), and heparan sulfate (Figure 1j). Immunoreactivities for these molecules were enhanced in the rimmed vacuoles and coarse granular structures in the affected muscle fibers of CM.

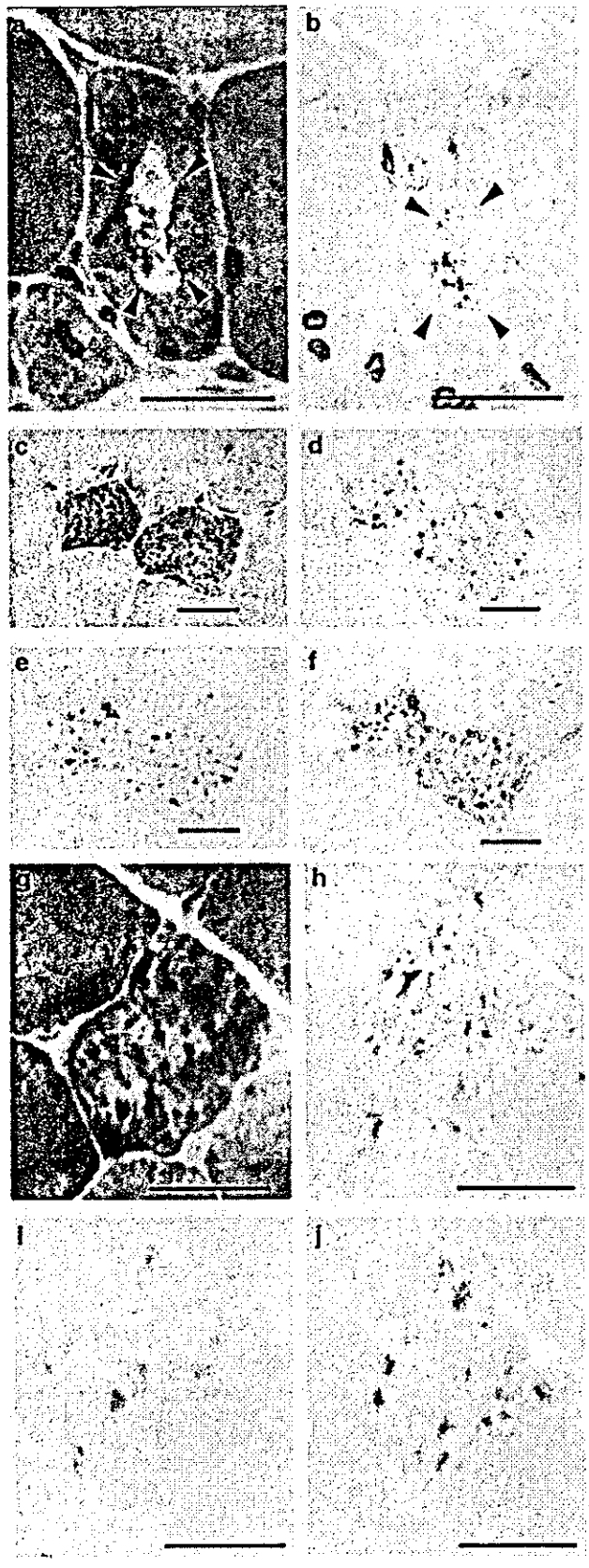

Figure 1 Immunohistochemical findings in CM muscles. Transverse sections of chloroquine-treated (50 mg/kg/day for 60 days) hamster soleus muscles are shown. (a) HE stain shows rimmed vacuole formation (arrow heads). (b) Immunoreactivity for PrP is detected in a rimmed vacuole (arrow heads) shown in (a). (c–f), (g–j) Serial sections stained with HE (c), modified Gomori trichrome (g), acid phosphatase (h), and immunostained for PrP (d), apolipoprotein J (e), clathrin (f), cathepsin B (i), and heparan sulfate (j). Scale bars = 20 μm.

PrP^{CQ} is Slightly Less Sensitive to PK Digestion

Western blot analysis using a polyclonal antibody PrP2B, raised against hamster PrP89-103, revealed prominent bands of 27 and 30 kDa in either CM muscular homogenates or the control, before digestion with PK. There was no significant difference in the intensity of PrP signals between CM muscles and controls (first lanes, Figure 2a, b). The specificity of these bands was confirmed by absorbing the PrP2B antibody with synthetic peptide PrP89-103 (Figure 2c). Although both of the PrP molecules were completely digested with 50 μg/ml of PK, which was the stringent condition to distinguish PrP^{Sc} from PrP^{C} (data not shown), digestion with a smaller amount of PK revealed different PK sensitivity between the PrP molecules from CM muscles (PrP^{CQ}) and PrP^{C} from the control muscles. PrP^{C} derived from control hamster muscle was apparently digested with 0.375 μg/ml of PK, whereas a considerable amount of PrP^{CQ} of 27 kDa still remained after treatment with 1.0 μg/ml of PK (Figure 2a and b). Statistical analysis of the relative density of the bands revealed a significant difference between PrP^{C} and PrP^{CQ} after treatment with 0.5, 0.75, or 1.0 μg/ml of PK (Figure 2d).

PrP^{CQ} is Partially Insoluble in Detergent

Western blot analysis using a monoclonal antibody 3F4 revealed prominent signals at 35 kDa and additional signals at about 30 kDa in the supernatants from either CM muscle homogenate or the control (first lanes, Figure 3a, b). While PrP^{C} from control muscle was completely solubilized in the lysis buffer containing 0.5% NP-40 (Figure 3a), a considerable amount of PrP^{CQ} remained in the

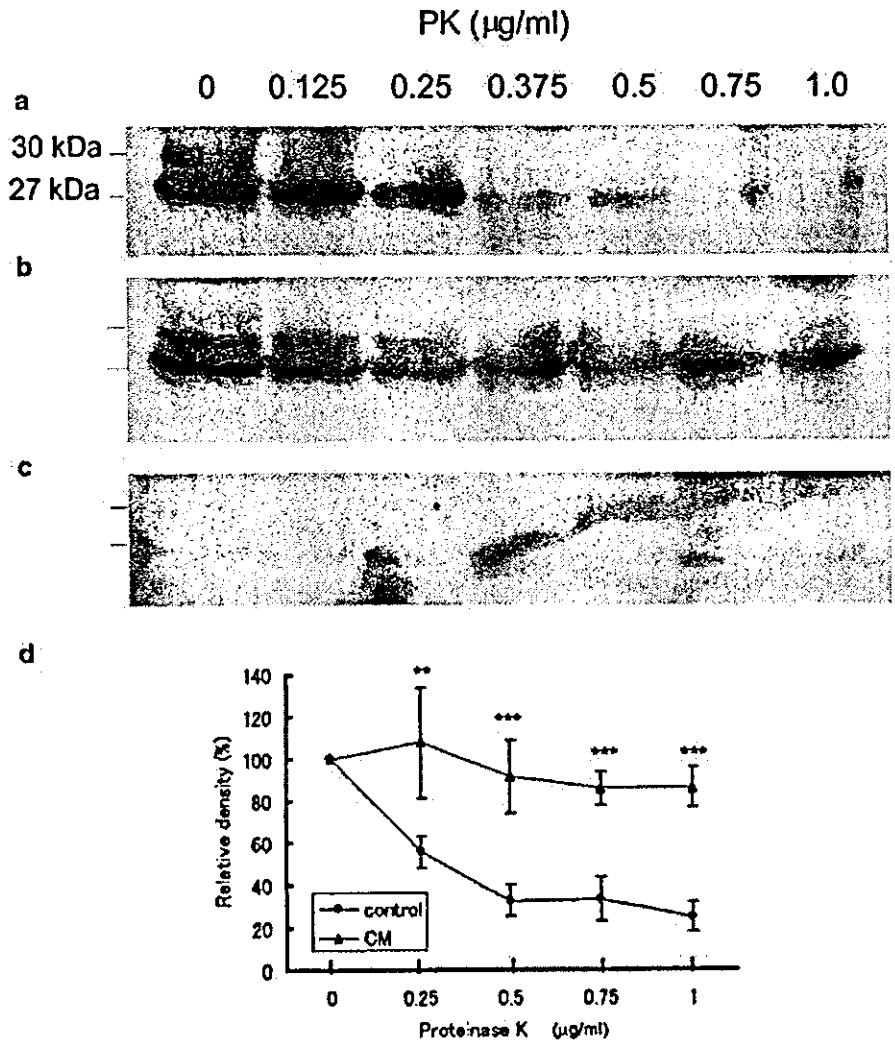

Figure 2 PK sensitivity of PrP molecules in CM muscles. (a–c) PrP molecules in the homogenate of control hamsters (a) or CM hamsters (b) were detected with PrP2B antibody after digestion with a designated amounts of PK at 37°C for 20 min. Prominent bands of 27 kDa and 30 kDa were diminished after the antibody had been absorbed by a synthetic polypeptide used for immunization (c). (d) Densitometric analysis of 27 and 30 kDa bands. Data from three independent experiments are indicated. $^{**}P<0.05$, $^{***}P<0.01$.

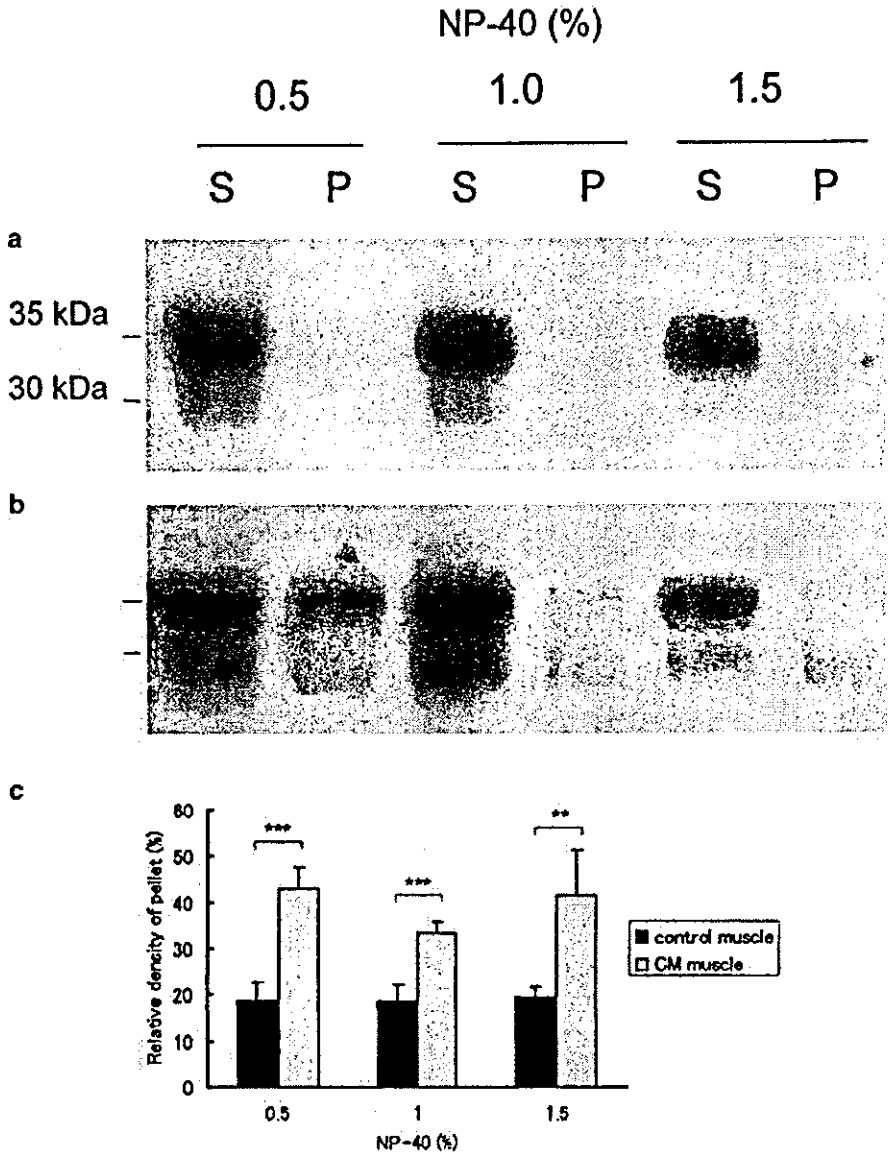

Figure 3 Solubility in NP-40 of PrP molecules in CM muscles. (a, b) Muscles from control hamsters (a) or CM hamsters (b) were homogenized in the lysis buffer containing designated amount of NP-40 and subsequently ultracentrifuged at 265 000 *g* to separate detergent-soluble PrP molecules in the supernatant (S) and detergent-insoluble molecules in the pellet (P). PrP molecules were labeled with 3F4 monoclonal antibody. (c) Relative PrP amount in the pellet fraction. Percentage of PrP signals (30 and 35 kDa) of the pellet fraction in the sum of those of the pellet and the supernatant is shown. Data from three independent experiments. $^{**}P<0.05$, $^{***}P<0.01$.

insoluble fraction in the presence of 0.5, 1.0, or 1.5% NP-40 (Figure 3b, c).

PrP^{CQ} is not Pathogenic

To investigate whether PrP^{CQ} is able to cause pathological changes characteristic of prion diseases *in vivo*, 10% muscular homogenates containing PrP^{CQ} were injected into the brain of Syrian hamsters. The hamsters were observed over 2 years after the inoculation had been given, and none of them developed any signs of prion diseases nor muscle disorders (data not shown). Histological examination of the brain revealed no significant pathological findings or abnormal PrP deposition (Figure 4).

Discussion

In this study, we have demonstrated that slightly less PK-sensitive and partially detergent-insoluble PrP^{CQ} accumulated in affected muscle fibers of experimental CM in hamsters. While PrP molecules from control muscle were sensitive to PK digestion at 0.375 μg/ml and fully soluble in buffer containing 0.5% NP-40, PrP^{CQ} molecules were less sensitive to PK digestion up to 1.0 μg/ml, and a considerable portion of them was insoluble in buffer containing

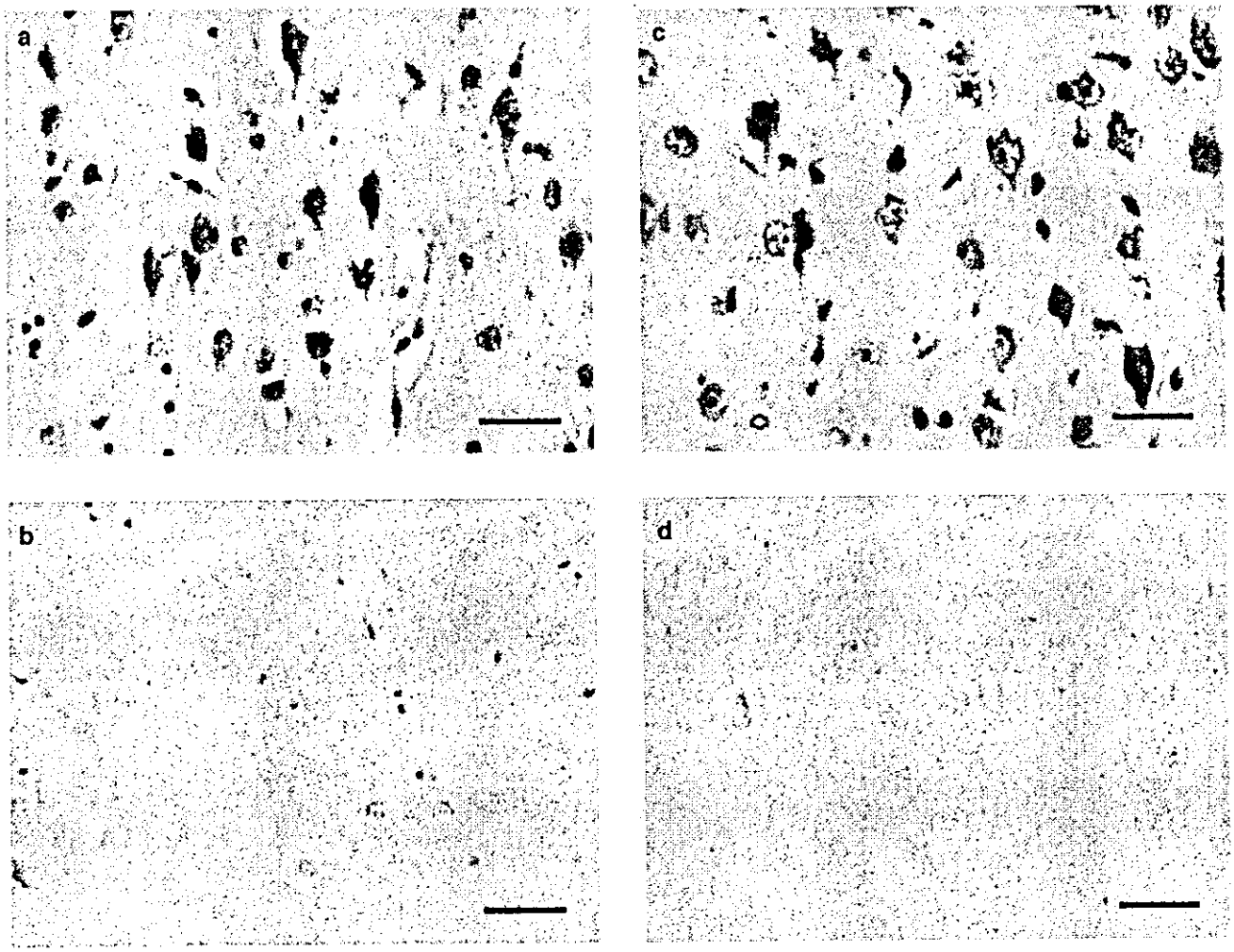

Figure 4 Histological analysis of hamster brain inoculated with CM muscle homogenate. Sections of the brain inoculated with PrP^{C}-containing muscle homogenate (**a**, **b**) or PrP^{CQ}-containing muscle homogenate (**c**, **d**) were stained with HE (**a**, **c**) or immunostained using 3F4 monoclonal antibody (**b**, **d**). Neither neurodegenerative change nor abnormal PrP deposition was revealed. Scale bars = 30 μm.

1.5% NP-40. These biochemical properties of PrP^{CQ} molecules are distinct from PrP^{C}.

There have been several attempts to create *de novo* PrP^{Sc}-like molecules *in vitro*. Using a cell-free conversion system, Horiuchi *et al*[13] were able to convert PrP^{C} into a protease-resistant isoform by the addition of PrP^{Sc} under physiological conditions. Even in the absence of PrP^{Sc}, an acidic buffer can give a β-sheet-dominant conformation and PK resistance to PrP^{C} *in vitro*.[14,15] Nevertheless, no *de novo* PrP^{Sc}-like molecules succeeded to reproduce the disease *in vivo*.[16] In the present study, PrP^{CQ} molecules were not capable of causing any pathological changes in the central nervous system. PrP^{CQ} molecules seem to be distinct from both of these *de novo* PrP^{Sc}-like molecules and PrP^{Sc}, because PrP^{CQ} molecules possess neither marked resistance to PK and detergent insolubility nor transmissibility of the disease conditions.

The CM model reported in this study is different from other PrP-conversion models previously reported, in that PrP^{CQ} molecule was generated *in vivo* in the absence of exogenous input of PrP^{Sc} or PrP^{Sc}-like molecules. Instead, the microenvironment in the lysosome was altered in hamsters by the injection of chloroquine to produce this distinct PrP molecule. Lysosomes are acidic compartments that have been reported to play an important role in the conformational conversion of PrP in prion diseases.[17,18] Chloroquine raises intralysosomal pH to as high as 6.0–6.5, causing marked changes in intracellular protein processing and trafficking.[8] As a consequence of the long-term administration of chloroquine, skeletal muscle fibers degenerate, with numerous autophagic vacuoles.[9] In the process of forming autophagic vacuoles, endogenous muscular PrP^{C} could acquire the properties of PrP^{CQ}.

In the present study, it remains unclear whether chloroquine modifies PrP^{C} molecules directly or indirectly. A previous study revealed that chloroquine does not directly interact with PrP molecules in scrapie-infected neuroblastoma cells.[19]

Furthermore, it has been reported that unfolded recombinant human prion protein PrP90-231 forms a stable protein folding intermediate rich in β-sheet at pH lower than 4.[14] Matsunaga *et al*[20] reported that pH is a crucial factor in determining the conformational state of some amyloidgenic proteins. They found that synthetic Aβ42 and stefin B peptides, showing similar amino-acid alignment to PrP90-144, tend to form amyloid fibrils at acidic pH. Considering these observations, it is unlikely that chloroquine directly interacts with PrP^{C} molecules. An increase in lysosomal pH due to chloroquine, and subsequent metabolic changes in lysosomal systems might be responsible for the biosynthesis of PrP^{CQ} molecules.

Besides experimental CM, there are a few experimental models in which PrP molecules of skeletal muscle are rendered partially PK-resistant and detergent-insoluble. Chiesa *et al*[21] established transgenic mice expressing PrP molecules with nine-octapeptide insertional mutation. Mutated PrP molecules obtained PrP^{Sc}-like properties in the brain and the periphery, producing neurodegeneration similar to an inherited prion disease in humans. In their model, the primary structure of PrP molecules was changed and the mutated PrP was overexpressed not only in the brain but also in the skeletal muscle and heart. This model is quite different from our CM model, in that the primary structure of PrP molecules was not manipulated.

The other experimental model is a transgenic mouse harboring high copy numbers of wild-type PrP transgenes, which spontaneously exhibited necrotizing myopathy, demyelinating polyneuropathy, and focal vacuolation of the central nervous system without apparent deposition of PrP^{Sc}.[22] In spite of severe neurodegeneration and neuromyopathy, only small amount of PK-resistant PrP was detected in affected muscles and brains. They concluded that low level of PK-resistant PrP might reflect aggregation of PrP^{C} and was not correlated with neuropathological changes in these transgenic mice. In our study, PrP^{CQ} after PK digestion did not show molecular characteristics of PrP^{Sc} in prion diseases, suggesting that PrP^{CQ} acquires less PK sensitivity through a different mechanism from that of PrP^{Sc}. Although the expression level of PrP was not increased in CM (data not shown), it is possible that distinct biochemical properties of PrP^{CQ} might simply be due to protein aggregation or alteration in PK–protein ratio, not to the conformational change of monomeric PrP^{C} molecules.

PrP^{CQ} in the affected muscles of the present model was accompanied by the accumulation not only of lysosomal markers but also of those molecules known to be involved in prion disease pathogenesis, such as clathrin, heparan sulfate proteoglycan, and apolipoprotein J.[23–25] It is known that certain sulfated glycans, such as heparan sulfate and pentosan polysulfate, stimulate PrP conversion *in vitro*.[26] Then, it might be possible that accumulated heparan sulfate in the CM muscles contribute to the acquisition of altered PK sensitivity and partial detergent insolubility of the PrP molecules.

Experimental CM in the rat has been established previously as a model of myopathies with rimmed vacuoles, including distal myopathy with rimmed vacuole formation and inclusion-body myositis. Owing to of the deposition of amyloid β in inclusion-body myositis,[27] experimental CM has been utilized by several groups as a peripheral model to investigate the pathogenesis of Alzheimer's disease.[10,28] The precise mechanism of rimmed vacuole formation in CM is still unknown; however, it has been reported that chloroquine causes an increase in endogenous autophagosomes in mammalian cells.[29] Similar mechanism(s) might be shared between amyloid β deposition in the CM rat model and PrP^{CQ} accumulation in our CM hamster model.

The PrP2B polyclonal antibody revealed prominent 27 kDa signals with additional 30 kDa signals (Figure 2), while the 3F4 monoclonal antibody reacted with dominant 35 kDa signals and additional 30 kDa signals (Figure 3), which were similar to Cp33-37 signal in skeletal muscle of hamster.[30] The common signals of 30 kDa were detected by both of the two antibodies. Minor epitope differences between the two antibodies might account for such a diversity of PrP signals, but it remains to be elucidated.

Finally, together with the biochemical and biological properties of PrP^{CQ}, the immunohistochemical findings in CM muscles of the molecules known to be involved in prion disease pathogenesis indicate that experimental CM in hamsters is a useful *in vivo* model to investigate the mechanism of PrP accumulation in the pathogenesis of PrP-related diseases.

Acknowledgements

We are grateful to Professor Mitsuo Takahashi at Fukuoka University and Professor Masami Niwa at Nagasaki University for their critique and suggestions on the research and this report. The English used in this manuscript was revised by Universal Academy Press, Inc., Japan.

This work was supported by a grant (H13-kokoro-025) to KD from the Ministry of Health, Labor and Welfare of Japan.

References

1 Prusiner SB. Molecular biology of prion diseases. Science 1991;252:1515–1522.
2 Hill AF, Zeidler M, Ironside J, *et al.* Diagnosis of new variant Creutzfeldt-Jakob disease by tonsil biopsy. Lancet 1997;349:99–100.
3 Glazel M, Abela E, Maisson M, *et al.* Extraneural pathologic prion protein in sporadic Creutzfeldt–Jakob disease. N Eng J Med 2003;349:1812–1820.

4 Bosque PJ, Ryou C, Telling G, *et al.* Prions in skeletal muscle. Proc Natl Acad Sci USA 2002;99:3812–3817.
5 Frederikse PH, Zigler Jr SJ, Farnsworth PN, *et al.* Prion protein expression in mammalian lenses. Curr Eye Res 2000;20:137–143.
6 Askanas V, Bilak M, Engel WK, *et al.* Prion protein is abnormally accumulated in inclusion-body myositis. Neuroreport 1993;5:25–28.
7 Zanusso G, Vattemi G, Ferrari S, *et al.* Increased expression of the normal cellular isoform of prion protein in inclusion-body myositis, inflammatory myopathies and denervation atrophy. Brain Pathol 2001;11:182–189.
8 Holzman E. Lysosomes. Cellular organelles. Plenum Press: New York and London, 1989.
9 Macdonald RD, Engel AG. Experimental chloroquine myopathy. J Neuropath Exp Neurol 1970;29:479–499.
10 Tsuzuki K, Fukatsu R, Takamaru Y, *et al.* Co-localization of amyloid-associated proteins with amyloid beta in rat soleus muscle in chloroquine-induced myopathy: a possible model for amyloid beta formation in Alzheimer's disease. Brain Res 1995;699:260–265.
11 Kitamoto T, Shin RW, Doh-ura K, *et al.* Abnormal isoform of prion protein accumulates in the synaptic structures of the central nervous system in patients with Creutzfeldt–Jakob disease. Am J Path 1992;140: 1285–1294.
12 Lehmann S, Harris DA. Blockade of glycosylation promotes acquisition of scrapie-like properties by the prion protein in cultured cells. J Biol Chem 1997; 272:21479–21487.
13 Horiuchi M, Caughey B. Specific binding of normal prion protein to the scrapie form via a localized domain initiates its conversion to the protease-resistant state. EMBO J 1999;18:3193–3203.
14 Swietnicki W, Peterson R, Gambetti P, *et al.* pH-dependent stability and conformation of the recombinant human prion protein PrP(90-231). J Biol Chem 1997;272:27517–27520.
15 Matsunaga Y, Peretz D, Williamson A, *et al.* Cryptic epitope in N-teminally truncated prion protein are exposed in the full-length molecule: dependence of conformation on pH. Proteins 2001;44:110–118.
16 Hill AF, Antoniou M, Collinge J. Protease-resistant prion protein produced *in vitro* lacks detectable infectivity. J Gen Virol 1999;80:11–14.
17 Laszlo L, Lowe J, Self T, *et al.* Lysosomes as key organelles in the pathogenesis of prion encephalopathies. J Pathol 1992;166:333–341.
18 Shyng SL, Huber MT, Harris DA. A prion protein cycles between the cell surface and an endocytic compartment in cultured neuroblastoma cells. J Biol Chem 1993;268:15922–15928.
19 Doh-ura K, Iwaki T, Caughey B. Lysosomotropic agents and cysteine protease inhibitors inhibit scrapie-associated prion protein accumulation. J Virol 2000;74:4894–4897.
20 Matsunaga Y, Zerovnik E, Yamada T, *et al.* Conformational changes preceding amyloid-fibril formation of amyloid-beta and stefin B: parallels in pH dependence. Curr Med Chem 2002;9:1717–1724.
21 Chiesa R, Pestronk A, Schmidt RE, *et al.* Primary myopathy and accumulation of PrPSc-like molecules in peripheral tissues of transgenic mice expressing a prion protein insertional mutation. Neurobiol Dis 2001;8:279–288.
22 Westaway D, DeArmond SJ, Cayetano-Canlas J, *et al.* Degeneration of skeletal muscle, peripheral nerves, and the central nervous system in transgenic mice overexpressing wild-type prion proteins. Cell 1994; 76:117–129.
23 Mouillet-Richard S, Ermonval M, Chebassier C, *et al.* Signal transduction through prion protein. Science 2000;289:1925–1928.
24 McBride PA, Wilson MI, Eikeleboom P, *et al.* Heparan sulfate proteoglycan is associated with amyloid plaques and neuroanatomically targeted PrP pathology throughout the incubation period of scrapie-infected mice. Exp Neurol 1998;149:447–454.
25 Sasaki K, Doh-ura K, Ironside JW, *et al.* Increased clusterin (apolipoprotein J) expression in human and mouse brains infected with transmissible spongiform encephalopathies. Acta Neuropathol (Berl) 2002;103: 199–208.
26 Wong C, Xiong LW, Horiuchi M, *et al.* Sulfated glycans and elevated temperature stimulate PrP^{Sc}-dependent cell-free formation of protease-resistant prion protein. EMBO J 2001;20:377–386.
27 Askanas V, Engel WK, Alvarez RB, *et al.* Beta-amyloid protein immunoreactivity in muscle of patients with inclusion-body myositis. Lancet 1992; 339:560–561.
28 Murakami N, Oyama F, Gu Y, *et al.* Accumulation of tau in autophagic vacuoles in chloroquine myopathy. J Neuropathol Exp Neurol 1998;57:664–673.
29 Suzuki T, Nakagawa M, Yoshikawa A, *et al.* The first molecular evidence that autophagy relates rimmed vacuole formation in chloroquine myopathy. J Biochem 2002;131:647–651.
30 Bendheim PE, Brown HR, Rudelli RD, *et al.* Nearly ubiquitous tissue distribution of the scrapie agent precursor protein. Neurology 1992;42:149–156.

Diffusion-weighted MRI abnormalities as an early diagnostic marker for Creutzfeldt–Jakob disease

Y. Shiga, MD, PhD; K. Miyazawa, MD; S. Sato, MD, PhD; R. Fukushima, MD; S. Shibuya, MD, PhD; Y. Sato, MD, PhD; H. Konno, MD, PhD; K. Doh-ura, MD, PhD; S. Mugikura, MD, PhD; H. Tamura, MD, PhD; S. Higano, MD, PhD; S. Takahashi, MD, PhD; and Y. Itoyama, MD, PhD

Abstract—*Objective:* To evaluate the usefulness of diffusion-weighted MRI (DWI) for the early diagnosis of Creutzfeldt–Jakob disease (CJD). *Methods:* Thirty-six consecutive patients (age 56 to 82 years) were enrolled, and 26 were examined by DWI. Nine were definite based on the World Health Organization criteria, and 27 were probable. The percentages of DWI abnormalities, periodic sharp wave complexes (PSWCs) on the EEG, detection of CSF 14-3-3 protein, and increase of CSF neuron-specific enolase (>25 ng/mL) on the first examination were compared. For DWI, 32 patients (age 31 to 84 years) who showed progressive dementia or impaired consciousness served as disease controls. *Results:* The percentage of DWI abnormalities was 92.3%, of PSWCs 50.0%, of 14-3-3 protein detection 84.0%, and of NSE increase 73.3%. Two of the 32 control subjects were falsely positive on DWI. The sensitivity of DWI was 92.3% (95% CI 74.8 to 99.5%) and specificity 93.8% (95% CI 79.2 to 99.2%). In 17 patients who did not show PSWCs on the first EEG, abnormal DWI findings were still clearly detected. Four patients who were negative for 14-3-3 protein also showed DWI abnormalities. DWI abnormalities were detected as early as at 3 weeks of symptom duration in four patients in whom PSWCs were not yet evident. *Conclusions:* DWI can detect characteristic lesions in the majority of patients with CJD regardless of the presence of PSWCs. DWI was the most sensitive test for the early clinical diagnosis of CJD; consideration should be given to its inclusion in the clinical diagnostic criteria of CJD.

NEUROLOGY 2004;63:443–449

Creutzfeldt–Jakob disease (CJD) is a transmissible, progressive, fatal spongiform encephalopathy.[1] The transmission of bovine spongiform encephalopathy to humans as variant CJD[2] has focused increased attention on CJD. The cardinal manifestations of the disease are rapidly progressive dementia, generalized myoclonus, and periodic sharp wave complexes (PSWCs) on EEG. However, cases that do not consistently show such typical manifestations have been recognized, and the spectrum of disease manifestations has been extending.[3,4] An early and accurate diagnosis is important to prevent disease transmission, but diagnosis is not easy, especially in the early stage of the disease.

PSWCs on EEG have been used as one of the central diagnostic tests for CJD.[5] However, PSWCs are observed in only 60% of patients[3,4] and usually appear after the middle stage of the disease. In addition, PSWCs are not always specific for CJD.[6] PSWCs are therefore of limited use for the early diagnosis of CJD. The detection of brain-specific proteins such as 14-3-3 protein[6] and neuron-specific enolase[7] (NSE) in CSF also supports the diagnosis of CJD. Although the sensitivity and specificity of 14-3-3 protein[6] and NSE[7] are higher than those of PSWCs,[8] false-positive results are observed in several neurologic diseases such as herpes simplex encephalitis, cerebrovascular disease,[6] Hashimoto encephalopathy,[9] and paraneoplastic neurologic disorders.[10]

Recently, several reports described that diffusion-weighted MRI (DWI) could demonstrate early brain lesions in CJD patients when scans were negative on T2-weighted MRI examination (T2I).[11] In this study, we evaluated the usefulness of DWI for the early clinical diagnosis of CJD by comparing it with other MR sequences such as T2I and fluid-attenuated inversion recovery imaging (FLAIR) and with other diagnos-

See also pages 410, 436, and 450

From the Department of Neurology (Drs. Shiga, Miyazawa, and Itoyama), Tohoku University School of Medicine, Department of Neurology (Dr. S. Sato), Kohnan Hospital, Second Department of Internal Medicine (Dr. Fukushima), Hiraka General Hospital, Department of Neurology (Dr. Shibuya), Miyagi National Hospital, Department of Neurology (Dr. Y. Sato), Research Institute for Brain and Blood Vessels, Akita, Department of Neurology (Dr. Konno), Nishitaga National Hospital, Department of Neuropathology (Dr. Doh-ura), Institute of Brain Diseases, Kyushu University Faculty of Medicine, and Department of Diagnostic Radiology (Drs. Mugikura, Tamura, Higano, and Takahashi), Tohoku University School of Medicine, Japan.

Presented in part at the 127th Annual Meeting of the American Neurologic Association, October 14, 2002, New York.

Received April 16, 2003. Accepted in final form March 18, 2004.

Address correspondence and reprint requests to Dr. Y. Shiga, Department of Neurology, Tohoku University School of Medicine, 1-1 Seiryo-machi, Aoba-ku, Sendai 980-8574, Japan; e-mail: yshiga@em.neurol.med.tohoku.ac.jp

Table 1 Profiles of CJD patients and examination results

Patient no.	Type	Age/sex	Duration, wk	DL	*PRNP*	PSWC	DWI	14-3-3	NSE, ng/mL
1	Sp	71/M	3	P	MM	−/+	+		
2	Sp	63/M	4	P	MM	+	+		26
3	Sp	78/M	6	P	MM	+	+	+	79
4	Sp	76/F	6	P	MM	+	+	−	22
5	Sp	61/M	7	P	MM	+	+	+	37.3
6	Sp	66/M	8	P	MM	−/+	+	+	29
7	Sp	76/F	8	P	MM	+	+	+	177
8	Sp	69/M	8	P	MM	+			
9	Sp	54/M	8	P	MM	−/+	+	+	18.4
10	Sp	69/M	8	D	VV2	−	+	+	110
11	Sp	68/M	9	P	MM	−/+	+	+	24
12	Sp	63/F	9	P	MM	+		+	56
13	Sp	74/M	10	D	MM	+			31
14	Sp	71/M	12	P	MM	+		+	25.2
15	Sp	63/F	12	P	MM	−/+	+	+	
16	Sp	79/M	13	D	MM	+		+	36
17	Sp	75/F	21	D	VV2	−	+	+	48
18	Sp	74/F	23	P	MM	+	+	+	51.4
19	Sp	59/M	24	D	MM2-T	−	−	−	15.4
20	Sp	73/F	25	P	MV	−	+	+	56.2
21	Sp	73/F	3	P		−/+	+		
22	Sp	69/M	3	P		−/+	+		50
23	Sp	67/F	6	P		+		+	95
24	Sp	70/M	8	P		+	−/+		
25	Sp	72/F	8	P		+			120
26	Sp	59/M	9	P		+	+		62
27	Sp	74/F	17	D		+		+	72
28	Sp	66/F	25	P		+		+	300
29	Fa	76/M	4	P	V1801	−	+	+	19.5
30	Fa	56/F	8	P	M232R	−/+	+	+	110
31	Fa	58/M	9	P	E200K	−/+	+		
32	Fa	72/M	12	D	V1801	−	+		60.4
33	Fa	82/F	13	P	V1801	−	+	+	32.1
34	Fa	79/M	24	D	V1801	−	+	−	13
35	Ia (Dura)	57/M	3	D	MM	−/+	+	−	18
36	Ia (Dura)	70/F	8	P		+		+	15.8

CJD = Creutzfeldt–Jakob disease; Duration, wk = duration from the onset to diagnostic examinations; DL = diagnostic level based on World Health Organization criteria; PSWC = periodic sharp wave complex; DWI = diffusion-weighted imaging; NSE = neuron-specific enolase; Sp = sporadic CJD; P = probable; MM = homozygosity for methionine at codon 129; D = definite; VV = homozygosity for valine at codon 129; MV = methionine/valine heterozygosity at codon 129; Fa = familial CJD; V180I = a point mutation of Val to Ile at codon 180; M232R = a point mutation of Met to Arg at codon 232; E200K = a point mutation of Glu to Lys at codon 200; Ia = iatrogenic CJD; Dura = a recipient of cadaveric dura mater; (−/+) = negative on the first examination but positive on the sequential examinations.

tic tests including PSWC, CSF 14-3-3 protein, and CSF NSE, which are used as the World Health Organization (WHO) CJD diagnostic criteria.[12]

Patients and methods. *Study group.* Thirty-six consecutive patients with CJD seen from January 1, 1994, to June 30, 2003, at the Department of Neurology, Tohoku University Hospital, and its related hospitals (age 56 to 82 years with a mean age of 68.9 years; 21 men) were enrolled in this study. These patients included the patients in our previous reports.[13-15] According to the WHO criteria,[12] 9 were definite and 27 were probable. A genetic study of human prion protein gene (*PRNP*) was performed in 27 patients, and 20 were sporadic CJD (17 had methionine homozygosity at codon 129 of *PRNP*, and, among those, 3 were definite; 14 were probable at the diagnostic level, and 2 who were definite had valine homozygosity and 1 who was probable had methionine/valine heterozygosity). Six had familial CJD (two definite, four probable, in which two had V180I[15] and one had E200K[16]; one had M232R).[17] Of two patients who were recipients of cadaveric dura mater (iatrogenic CJD), one was definite and one was probable (one had methionine homozygosity at codon 129 of *PRNP*). Our patients composed various clinical phenotypes of CJD including uncommon variants with rather longer clinical courses. The profiles of these patients are listed in table 1.

Disease control group. We reviewed retrospectively the clinical records of our patients who were admitted to the Department of Neurology, Tohoku University Hospital, from January 1, 1998, to June 30, 2003. Excluding patients who had an abrupt onset or symptoms suggesting meningoencephalitis, such as high fever, stiff neck, etc., 81 patients demonstrated subacute dementia or impaired consciousness progressing for 1 to several months.

Table 2 Final diagnosis of control patients

Final diagnosis	Total no.
Metabolic encephalopathy, including one alcoholic encephalopathy	4
Dementia with Lewy bodies	3
Corticobasal ganglionic degeneration	3
Cerebrovascular dementia	2
Viral encephalitis, including one herpes simplex encephalitis	3
Interval form of CO poisoning	3
Cryptococcal meningoencephalitis	2
Mitochondrial cytopathy	2
Progressive dementia, not otherwise specified	4
Alzheimer disease	1
CNS lymphoma	1
Multiple sclerosis	1
Temporal lobe epilepsy	1
Leukoencephalopathy, not otherwise specified	1
Ganser syndrome	1
Total	32

Thirty-two (age 31 to 84 years with a mean age of 61.9 years; 15 men) of 81 patients had undergone DWI examination. They served as disease controls for DWI because obtaining a large group of individuals with suspected CJD but with an alternative diagnosis was difficult. Of these patients, four had seriously suspected CJD, for whom the final diagnosis in two was metabolic encephalopathy that was improved by IV vitamin administration, one was mitochondrial encephalopathy as confirmed by an enzyme assay, and one was corticobasal ganglionic degeneration verified by autopsy. These controls included dementia with Lewy bodies, Alzheimer disease (AD), cerebrovascular disease, CNS infection, metabolic or mitochondrial encephalopathy, CNS malignancy, corticobasal ganglionic degeneration, interval form of CO intoxication, etc. Dementia with Lewy bodies, AD, and cerebrovascular disease are major differential diagnoses of CJD,[18] and CNS infection, encephalopathy, and CNS malignancy sometimes demonstrate positive 14-3-3 protein test in CSF,[19] which is an important diagnostic marker for CJD.[6] The disease controls are listed in table 2.

We compared the sensitivities of the positive results of MR sequences such as DWI, T2I, and FLAIR. We also assessed interobserver agreement. We compared the sensitivities of the positive results of DWI, PSWC, and brain-specific proteins such as 14-3-3 protein and NSE in CSF for making a diagnosis of CJD. PSWC and positive assay of 14-3-3 protein are included in the WHO diagnostic criteria.[12] These examinations were carried out 3 to 25 weeks after the onset with a mean duration of 10.7 weeks after the onset (see table 1).

Methods. DWI technique. Scans were performed on a number of units. A 1.5 or 1.0 T MR unit (Signa Horizon LX, GE Medical Systems, Milwaukee, WI; or Magnetom Vision, Siemens, Erlangen, Germany) was used. DWI was performed in 26 CJD cases with single-shot spin-echo echo-planar imaging. Imaging parameters were as follows: 4,700 to 5,000/93 to 120/1 or 2 (repetition time/effective echo time/no. excitations), 10 to 15 axial sections of 5- or 6-mm section thickness with a 1.5- to 3.0-mm intersection gap, 128 × 128 matrix, 220- or 230-mm field of view, and a diffusion-encoding strength (b factor) of 1,000 s/mm^2. In 23 of 26 CJD cases, T2I was performed, and in 17 of 26 CJD cases, FLAIR was performed. DWI, T2I, and FLAIR were performed on the same day using the same MR unit.

MRI investigation. MRI scans were assessed retrospectively as hard copies by two well-experienced neuroradiologists blind to clinical information, who examined each type of sequence separately, without referring to the other MR sequences, independently and individually. We accepted three types of high-intensity lesions as CJD-related lesions on DWI: lesions in the striatum (caudate or putaminal or both), lesions in the thalamus including the pulvinar, and lesions along the cortical ribbon (cerebral or cerebellar). We also accepted the lesions of several types in combination. We accepted not only the symmetric lesions but also asymmetric or unilateral lesions. DWI scans of the disease control group were also assessed retrospectively as hard copies combined with five DWI scans of CJD patients by the same two neuroradiologists, completely blind to clinical information to minimize observer bias.

PSWCs. EEG was recorded using the International 10–20 System. PSWCs were defined as diffuse biphasic or triphasic sharp wave complexes with a duration between 100 and 600 milliseconds and an intercomplex interval between 500 and 2,000 milliseconds.[6]

Brain-specific proteins in CSF. 14-3-3 protein immunoassay in CSF by means of western blotting was performed using a polyclonal antibody to the β isoform of 14-3-3 protein, SC 629 (Santa Cruz Biotechnology, Santa Cruz, CA). The presence of the band against the antibody, SC 629, was investigated. NSE in CSF was measured commercially using an ELISA (SRL Laboratory, Tokyo, Japan), and a value of >25 ng/mL[20] was judged as positive.

Statistical analyses of the diagnostic sensitivities of DWI, PSWCs, and NSE and 14-3-3 protein in CSF, positive rate of DWI, T2I, and FLAIR, and interobserver agreement rate were done using the Fisher exact probability test.

Results. *MRI.* DWI was examined in 26 CJD patients 3 to 25 weeks after the onset with a mean duration of 10.7 weeks. Twenty-four CJD patients showed high-intensity brain lesions by DWI examination. For both observers, the sensitivity of DWI for the CJD diagnosis was 92.3%. The interobserver agreement rate was 100%. Three patients (12.5%) showed lesions only in the caudate heads and putamen, 10 (41.7%) patients showed linear lesions only in the cerebral cortex, and 11 (45.8%) patients showed lesions in both the basal ganglia and the cerebral cortex (figure 1). Among them, only three patients (12.5%) showed lesions in the thalamus. No patients showed high-intensity lesions in the cerebellum. High-intensity lesions on DWI appeared before brain atrophy. The lesions involving the striatum were not always symmetric at the beginning but later became symmetric (figure 2), although symmetric striatal lesions are well known in CJD.[11] In some cases, the high-intensity lesions with sequential DWI did not always progress with the advance of the disease, and the signal intensity sometimes decreased with the disease progression in some lesions. In some cases, the cortical high signal varied in intensity and anatomic distribution (figure 3). In the terminal stage with profound brain atrophy, the high-intensity lesions became unclear. T2I was examined in 23 of 26 DWI-examined patients, but one T2I scan was excluded because of the low quality due to motion artifacts. One observer judged that 11 of 22 patients were positive (50.0%), and another observer judged that 8 were positive (36.4%). The interobserver agreement rate was 68.2%, and it was lower than that of DWI ($p < 0.005$). In both observers, DWI was more sensitive than T2I ($p < 0.005$ for one observer and $p < 0.0005$ for another observer). FLAIR was examined in 17 of 26 patients. One observer judged that 10 of 17 patients were positive (58.8%), and another observer judged that 7 were positive (41.2%). The interobserver agreement rate was 82.4%, and this also was lower than that of DWI ($p < 0.05$). DWI was more sensitive than FLAIR ($p < 0.01$ for one observer and $p < 0.0005$ for another observer). We show in figure 4 an example in which only DWI could detect abnormal high-intensity lesions.

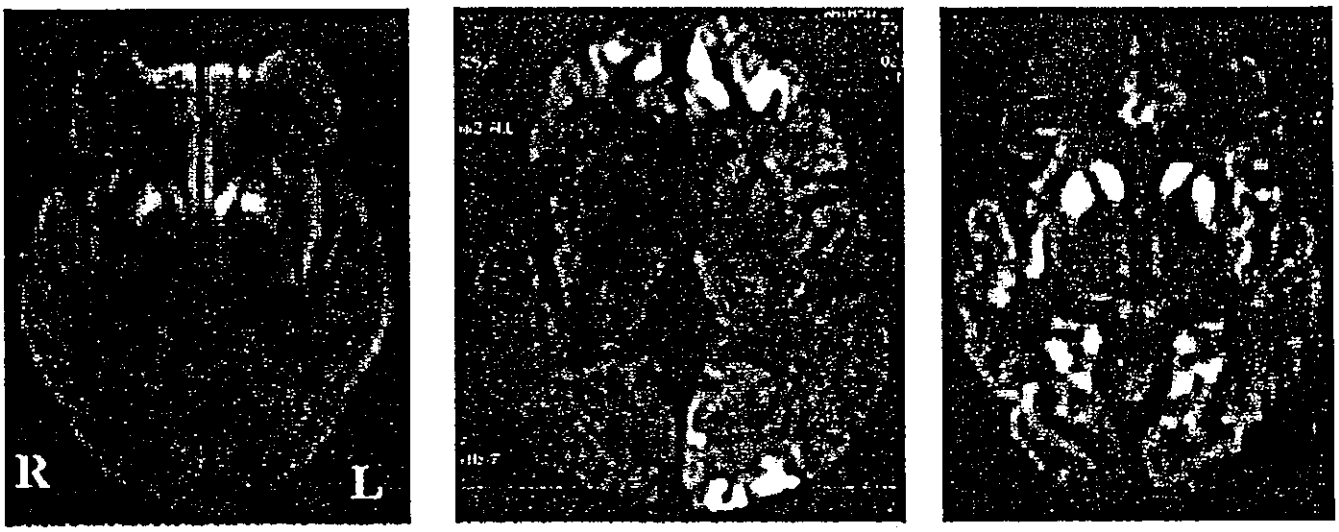

Figure 1. MRI changes seen in Creutzfeldt–Jakob disease. Three patterns of high-intensity lesions were seen: striatal lesion (A), cerebral cortical lesion (B), and a combination of both lesions (C).

DWI failed to detect any lesions in two patients at the first examination. The second DWI showed high-intensity lesions at the striatum in one of those patients. Repeated DWI scans of the other patient did not show any high-intensity lesions throughout his disease course. On the postmortem examination, protease-resistant type 2 prion protein was detected in this patient by western blot analysis using monoclonal antibody 3F4 (Signet Laboratories, Dedham, MA), and there were no spongiform changes. This case was classified as MM2-thalamic according to Parchi's classification (table 1).[3]

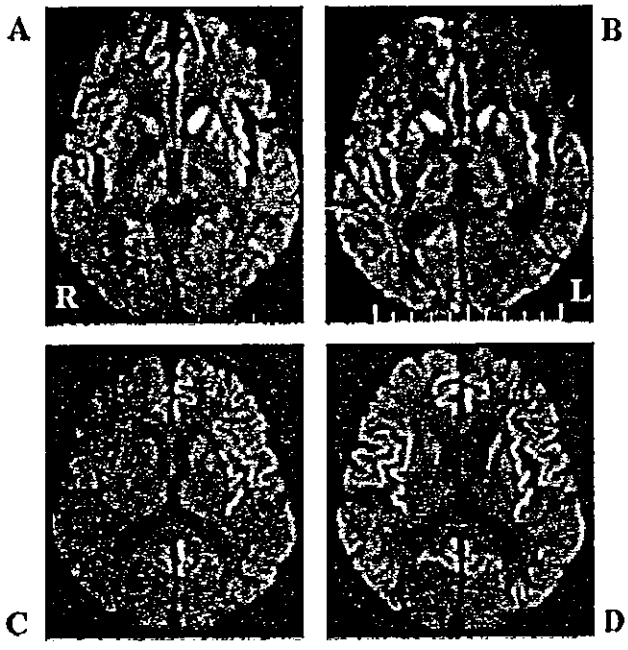

Figure 2. Chronologic change of the striatal and cortical lesions. A case of sporadic Creutzfeldt–Jakob disease (CJD) showing the progression of the basal ganglia signal changes from asymmetric (A) to symmetric (B). The interval between (A) and (B) was 2 months. A case of familial CJD with V180I mutation showing the progression of the cerebral cortex and caudate head signal changes from asymmetric (C) to symmetric (D). The interval between (C) and (D) was 4 months.

High-intensity DWI lesions that were in agreement with our criteria were observed in the disease control patients. One observer judged that a 69-year-old woman with cryptococcal meningoencephalitis and a 60-year-old woman with interval form of CO poisoning were falsely positive. Another observer judged that a 48-year-old woman with herpes simplex encephalitis and a 47-year-old with alcoholic encephalopathy were falsely positive. For both observers, the false-positive rate was 6.3% and the interobserver agreement rate was 87.5%. No highly CJD-suspected patients demonstrated high-intensity lesions. The sensitivity of DWI was 92.3% (95% CI 74.8 to 99.5%) and specificity 93.8% (95% CI 79.2 to 99.2%).

DWI detected the brain lesions before the appearance of PSWCs on EEG in 10 patients. DWI abnormalities were detected as early as at 3 weeks of symptom duration in four patients in whom PSWCs were not yet evident. In seven of eight patients who did not show PSWCs throughout their disease course, the first DWI clearly demonstrated the brain lesions (see table 1).

PSWCs on EEG. EEG was recorded from all 36 patients. Eighteen of 36 (50.0%) patients showed PSWCs that fit the criteria on the first EEG. In 10 of 18 PSWC-negative patients, sequential EEG showed PSWCs. However, eight patients (22.2%) did not show PSWCs in further sequential EEG recordings. The genetic analysis of *PRNP* demonstrated that four had a point mutation of V180I and one had MV at codon 129, and the postmortem examination revealed that two had VV2 and one had MM2-thalamic (see table 1). Generally, these types of CJD patients do not show PSWCs.[3]

Brain-specific proteins in CSF. The 14-3-3 protein was examined in 25 patients and NSE in 30. Twenty-one of those 25 patients (84.0%) were positive for 14-3-3 protein

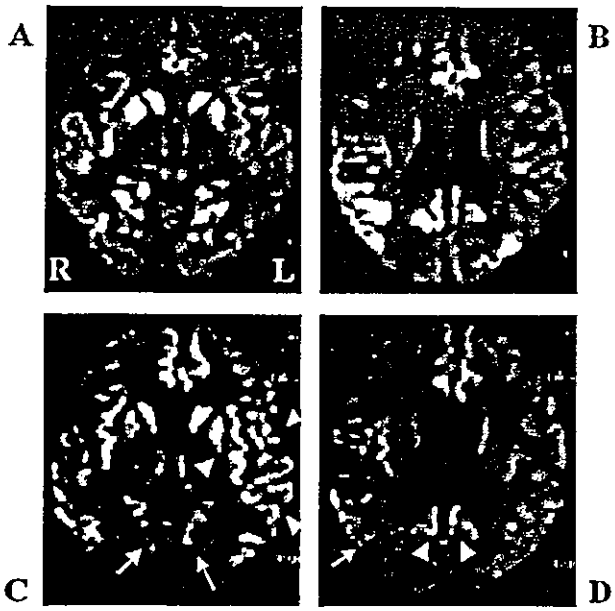

Figure 3. Chronologic change of the cortical lesions in sporadic Creutzfeldt–Jakob disease (sCJD). The cortical high intensity seen in a case of sCJD changed with time, with both increases and decreases in signal intensity in different areas. The high intensity in the bilateral occipital cortices (A) decreased (C, arrows), whereas the signal intensity in the left insular and temporal cortices (A) apparently increased (C, arrowheads). The interval between (A) and (C) was 1 month. The high intensity in the right temporal cortex and bilateral occipital cortices (B) decreased (D, arrow for the left temporal cortex and arrowheads for the bilateral medial occipital cortices). The interval between (B) and (D) was 1 month. Note that the high-intensity lesions depicted in diffusion-weighted imaging did not simply expand with the advance of the disease.

and 22 of those 30 patients (73.3%) were positive for NSE. In 24 patients examined for both brain-specific proteins, 16 were positive for both, 4 were negative for both, and 4 NSE-negative patients were positive for 14-3-3 protein (see table 1).

Comparison of sensitivity of DWI, PSWCs on EEG, and brain-specific CSF protein assay in diagnosing CJD. The sensitivity of DWI examined for the differential diagnosis was 92.3%, of PSWCs 50.0%, of 14-3-3 protein 84.0%, and of NSE 73.3%. DWI was more sensitive than PSWCs ($p < 0.0005$). 14-3-3 protein was more sensitive than PSWCs ($p < 0.01$). DWI tended to be more sensitive than 14-3-3 protein and NSE, but the differences were not significant ($p = 0.36$ and $p = 0.06$) (figure 5). In all 10 patients who had PSWCs in the sequential EEG recording, the lesions had already been detected earlier by DWI. DWI was positive in three of four 14-3-3 protein-negative patients and in six of seven NSE-negative patients. In only one patient who was classified as a rare variant of MM2-thalamic,[3] DWI, PSWC, 14-3-3 protein, and NSE were all negative.

Discussion. MRI had not been thought to be a sensitive noninvasive diagnostic test of CJD[21]; it was previously thought that EEG was the most reliable diagnostic test.[5] Increased signal intensity in the basal ganglia on T2I was first described in 1988,[22] and it was demonstrated that MRI was useful in depicting the lesions of CJD.[23] Although the usefulness of DWI for the early diagnosis of CJD has been suggested,[11,13] no one has compared the ability to depict the lesions among MR sequences such as T2I, FLAIR, and DWI or the accuracy of DWI in diagnosing CJD, especially for the early clinical diagnosis of CJD, with other noninvasive tests including EEG. In this study, we found that the sensitivity of DWI was 92.3% and that DWI was significantly more sensitive than conventional T2I and FLAIR in detecting the CJD-related lesions. T2I and FLAIR, whose sensitivities were 40 to 50%, are inadequate as a test for the first-line differential diagnosis. Further, the CJD-related lesions that we demonstrated on DWI were not detected in a small number of controls with AD, dementia with Lewy bodies, and cerebrovascular dementia, which are the major differential diagnoses of CJD.[18] We have demonstrated the superiority of DWI over the other noninvasive diagnostic tests by comparing its sensitivity with that of PSWCs on EEG, 14-3-3 protein, and NSE examined for the differential diagnosis. Unexpectedly, the interobserver agreement rate of DWI was 100%, and it was significantly higher than that of T2I and FLAIR. This indicates that DWI, which can depict the CJD-related lesions clearly and reliably, may represent a very important diagnostic test for the differential diagnosis. As we demonstrated previously,[13] DWI is more tolerant of motion artifacts than T2I and FLAIR. This advantage is especially important in CJD patients with the involuntary movement of myoclonic jerk. This tolerance may be one of the reasons for the higher sensitivity and the higher interobserver agreement rate of DWI compared with T2I and FLAIR.

The positive rates of T2I by our two observers were 36.4 and 50.0%, and these were significantly lower than a previously reported positive rate for T2I of 79.3%.[23] We think that this discrepancy can be accounted for by the difference in the time when the MRI was examined; the mean duration for our patients from the onset to MRI examination was 10.7 weeks (2.6 months), whereas that of the previous report was 8.1 months.[23] A positive rate for T2I of 67.3% was also reported; however, the positive rate of the first T2I in that report was 43.2%.[24] This is almost the same as in our results.

Currently, PSWCs play a central role in the diagnosis of CJD.[12] However, in the case of PSWC-negative patients, the diagnosis of CJD is sometimes difficult, and such cases are classified as "possible CJD."[12] We have demonstrated in this study not only that DWI was positive earlier than the presence of PSWCs but also that DWI was positive in CJD subjects without PSWCs throughout their disease. In the suspected CJD patients who are diagnosed as "possible CJD," the accuracy of the diagnosis is different between DWI-positive patients and DWI-negative patients. The likelihood of CJD is higher in

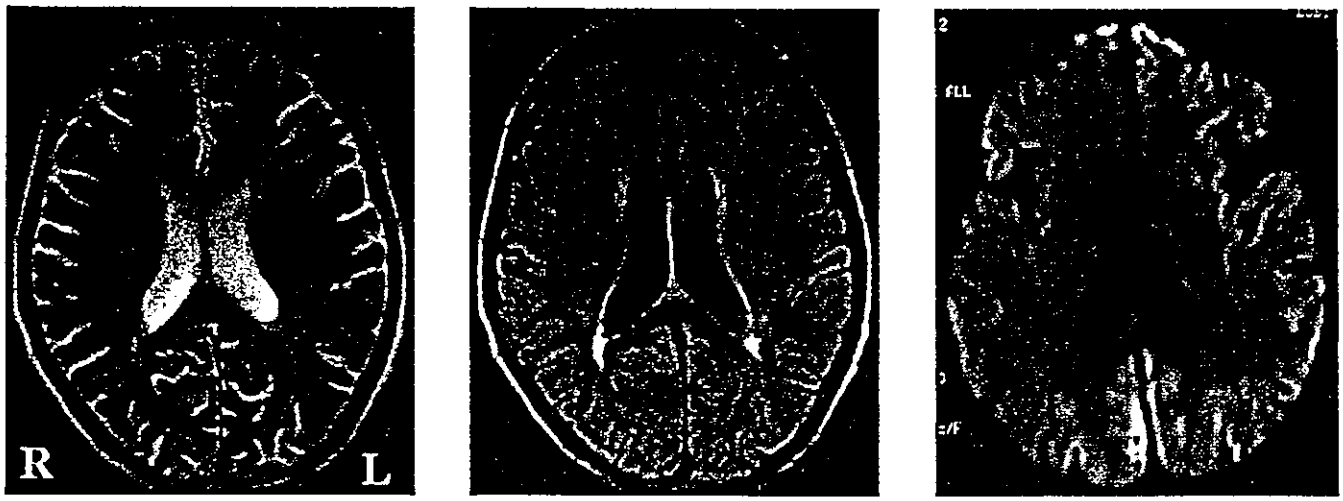

Figure 4. Comparison of conspicuity of Creutzfeldt–Jakob disease–related changes of the same patient on different MRI sequences. T2-weighted imaging (A) and fluid-attenuated inversion recovery imaging (B) show normal findings, and diffusion-weighted MRI (C) demonstrates high-intensity lesions in the cerebral cortex.

DWI-positive patients and lower in DWI-negative patients.

Each observer judged as false positive 2 of 32 disease controls. However, two observers did not agree on the result: one observer judged DWI of cryptococcal meningoencephalitis and interval form of CO poisoning as false positive, and another observer judged DWI of herpes simplex encephalitis and alcoholic encephalopathy as false positive. However, a careful history taking and the presence of pleocytosis in the CSF study significantly reduced the possibility of CJD. DWI was very useful to distinguish CJD from AD, vascular dementia, and dementia with Lewy bodies, which are the major differential diagnoses of CJD[18] and account for the vast majority of dementia in elderly patients.[25] DWI of mitochondrial encephalopathy, lactic acidosis, and stroke-like episodes (MELAS), Wilson disease, and Wernicke encephalopathy can demonstrate similar abnormalities. However, the clinical course and laboratory findings easily distinguish them from CJD. DWI in hypoglycemia,[26] anoxia,[27] and reversible posterior leukoencephalopathy syndrome[28] has also been reported to demonstrate high-intensity lesions similar to those of CJD. However, these have peculiar episodes, and the onset is apparently different from that of CJD. We must mention a 15-year-old boy with a final diagnosis of CNS lupus who was referred to the Japanese CJD Surveillance Committee. His consciousness disturbance developed subacutely, and his DWI showed scattered high-intensity lesions in the cerebral cortex and basal ganglia. His neurologic symptoms improved after the administration of prednisolone. CNS vasculitic disease also needs to be excluded in the differential diagnosis.

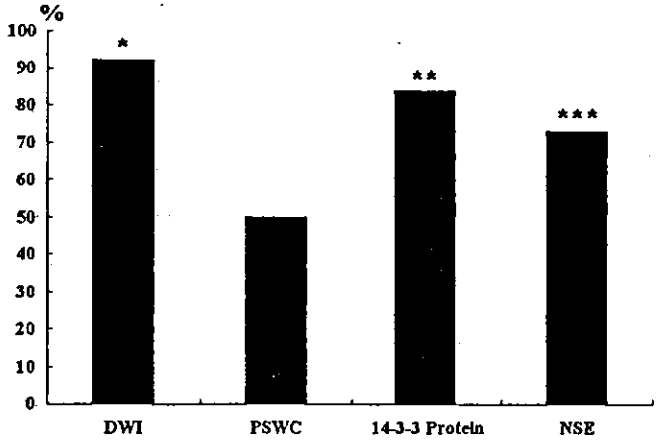

*Figure 5. Percentage of Creutzfeldt–Jakob disease cases with positive test. The positive rates of diffusion-weighted MRI (DWI), periodic sharp wave complexes (PSWCs), 14-3-3 protein, and neuron-specific enolase (NSE) examined for the differential diagnosis were 92.3, 50.0, 84.0, and 73.3%. *DWI was more sensitive than PSWCs ($p < 0.0005$). **14-3-3 protein was more sensitive than PSWCs ($p < 0.01$). *DWI tended to be more sensitive than 14-3-3 protein ($p = 0.36$) and NSE ($p = 0.06$). ***NSE tended to be more sensitive than PSWCs ($p = 0.053$). However, these were not significant.*

The kinds of pathologic findings that correlate with the CJD-related high-intensity lesions demonstrated in DWI are still controversial. Spongiform changes[29] and prion protein deposits[30] are candidates. The time lag from DWI examination to postmortem pathologic examination impedes an accurate understanding. The postmortem examination in one case of familial CJD with V180I whose DWI showed prominent high intensity in the cerebral cortex revealed severe spongiform changes and rather weak prion protein staining there immunohistochemically. The postmortem examination in a patient with spo-

radic CJD with MM2-thalamic whose DWI demonstrated negative findings throughout the disease course revealed no spongiform changes and rather weak prion protein staining. Based on our limited experience, we speculate that the high-intensity lesions depicted by DWI are related to spongiform changes rather than to prion protein deposition; however, more animal and postmortem studies are required to confirm this. It remains unclear why some high-intensity lesions become less prominent with the advance of the disease. We need to accumulate radiopathologic studies for several types of CJD.

The weaknesses of this study are that the number of ideal controls, CJD suspects with a final alternative diagnosis, was too small, because it was difficult to obtain a large number of such patients, and also the lack of pathologic diagnosis in the majority of CJD patients, with the result that only 9 of 36 patients were definite because of the difficulty in obtaining a postmortem examination in many cases. To overcome these weak points, a multicenter analysis of pathologically verified CJD patients and ideal controls is needed.

Last, in interpreting the results of the diagnostic tests, we must understand that such laboratory tests as DWI, brain-specific protein, and EEG reflect different aspects of the disease. Brain-specific proteins reflect the ongoing rapid and massive destruction of the neurons, and EEG reflects the current state of the injured brain.

Acknowledgment

The authors thank Drs. Keiji Chida, Nobuyuki Sato, Reiko Fukatsu, Takanori Oikawa, Hiroshi Kuroda, Takafumi Hasegawa, Atsushi Takeda, Akio Kikuchi, Naoki Suzuki, Masahiro Asano, and Kazutaka Jin for the patients' care. They also thank Dr. Tetsuyuki Kitamoto for analyzing the prion protein gene and Mr. Brent Bell for reading the manuscript.

References

1. Masters CL, Harris JO, Gadujeck DC, et al. Creutzfeldt–Jakob disease: patterns of worldwide occurrence and the significance of familial and sporadic clustering. Ann Neurol 1979;5:177–188.
2. Will RG, Ironside JW, Zeidler M, et al. A new variant of Creutzfeldt–Jakob disease in the UK. Lancet 1996;347:921–925.
3. Parchi P, Giese A, Capellari S, et al. Classification of sporadic Creutzfeldt–Jakob disease based on molecular and phenotypic analysis of 300 subjects. Ann Neurol 1999;46:224–233.
4. Zerr I, Schulz-Schaeffer WJ, Giese A, et al. Current clinical diagnosis in Creutzfeldt–Jakob disease: Identification of uncommon variants. Ann Neurol 2000;48:323–329.
5. Steinhoff BJ, Räcker S, Herrendorf G, et al. Accuracy and reliability of periodic sharp wave complexes in Creutzfeldt–Jakob disease. Arch Neurol 1996;53:162–166.
6. Zerr I, Bodemer M, Gefeller O, et al. Detection of 14-3-3 protein in the cerebrospinal fluid supports the diagnosis of Creutzfeldt–Jakob disease. Ann Neurol 1998;43:32–40.
7. Zerr I, Bodemer M, Räcker S, et al. Cerebrospinal fluid concentration of neuron-specific enolase in diagnosis of Creutzfeldt–Jakob disease. Lancet 1995;345:1609–1610.
8. Zerr I, Pocchiari M, Collins S, et al. Analysis of EEG and CSF 14-3-3 proteins as aids to the diagnosis of Creutzfeldt–Jakob disease. Neurology 2000;55:811–815.
9. Echebarria H, Saiz A, Graus F, et al. Detection of 14-3-3 protein in the CSF of a patient with Hashimoto's encephalopathy. Neurology 2000;54: 1539–1540.
10. Saiz A, Graus F, Dalmau J, et al. Detection of 14-3-3 protein in the cerebrospinal fluid of patients with paraneoplastic neurological disorders. Ann Neurol 1999;46:774–777.
11. Bahn MM, Parchi P. Abnormal diffusion-weighted magnetic resonance images in Creutzfeldt–Jakob disease. Arch Neurol 1999;56:577–583.
12. Zeidler M, Gibbs CJ Jr, Meslin F. WHO manual for strengthening diagnosis and surveillance of Creutzfeldt–Jakob disease. Geneva: World Health Organization, 1998:47–51.
13. Murata T, Shiga Y, Higano S, et al. Conspicuity and evolution of lesions in Creutzfeldt–Jakob disease at diffusion-weighted imaging. AJNR Am J Neuroradiol 2002;23:1164–1172.
14. Fukushima R, Shiga Y, Nakamura M, et al. MRI characteristics of sporadic CJD with valine homozygosity at codon 129 of the prion protein gene and PrPSc type 2 in Japan. J Neurol Neurosurg Psychiatry 2004;75:485–487.
15. Jin K, Shiga Y, Shibuya S, et al. Clinical features of Creutzfeldt–Jakob disease with V180I mutation. Neurology 2004;62:502–505.
16. Inoue I, Kitamoto T, Doh-ura K, et al. Japanese family with Creutzfeldt–Jakob disease with codon 200 point mutation of the prion protein gene. Neurology 1994;44:299–301.
17. Satoh A, Goto H, Satoh H, et al. A case of Creutzfeldt–Jakob disease with a point mutation at codon 232: Correlation of MRI and neurologic findings. Neurology 1997;49:1469–1470.
18. UK Creutzfeldt–Jakob Disease Surveillance Unit. Creutzfeldt–Jakob disease surveillance in the UK eleventh annual report 2002. 2003.
19. Lamstra AW, van Meegen MT, Vreyling JP, et al. 14-3-3 testing in diagnosing Creutzfeldt–Jakob disease. A prospective study in 112 patients. Neurology 2000;55:514–516.
20. Beaudry P, Cohen P, Brandel JP, et al. 14-3-3 protein, neuron-specific enolase, and S-100 protein in cerebrospinal fluid of patients with Creutzfeldt–Jakob disease. Dement Geriatr Cogn Disord 1999;10:40–46.
21. Zeidler M, Will RG, Ironside JW, et al. Magnetic resonance imaging is not a sensitive test for Creutzfeldt–Jakob disease. Br Med J 1996;312:844.
22. Gertz HJ, Henkes H, Cervos-Navvaro J. Creutzfeldt–Jakob disease: correlation of MRI and neuropathologic findings. Neurology 1988;38: 1481–1482.
23. Finkenstaedt M, Szudra A, Zerr I, et al. MR imaging of Creutzfeldt–Jakob disease. Radiology 1996;199:793–798.
24. Schröter A, Zerr I, Henkel H, et al. Magnetic resonance imaging in the clinical diagnosis of Creutzfeldt–Jakob disease. Arch Neurol 2000;57: 1751–1757.
25. McKeith IG, Galasko D, Kosaka K, et al. Consensus guidelines for the clinical and pathologic diagnosis of dementia with Lewy bodies (DLB): Report of the Consortium on DLB International Workshop. Neurology 1996;47:1113–1124.
26. Finelli PF. Diffusion-weighted MR in hypoglycemic coma. Neurology 2001;57:933–935.
27. Arbelaez A, Castillo M, Mukherji SK. Diffusion-weighted MR imaging of global cerebral anoxia. AJNR Am J Neuroradiol 1999;20:999–1007.
28. Mukherjee P, McKinstry RC. Reversible posterior leukoencephalopathy syndrome: evaluation with diffusion-weighted MR imaging. Radiology 2001;219:756–765.
29. Mittal S, Farmer P, Kalina P, et al. Correlation of diffusion-weighted magnetic resonance imaging with neuropathology in Creutzfeldt–Jakob disease. Arch Neurol 2002;59:128–134.
30. Haïk S, Dormont D, Fandeux BA, et al. Prion protein deposits match magnetic resonance imaging signal abnormalities in Creutzfeldt–Jakob disease. Ann Neurol 2002;51:797–799.

Journal of General Virology (2004), 85, 3449–3457 DOI 10.1099/vir.0.80043-0

Propagation of a protease-resistant form of prion protein in long-term cultured human glioblastoma cell line T98G

Yutaka Kikuchi,[1] Tomoshi Kakeya,[1] Ayako Sakai,[1] Kosuke Takatori,[1] Naoto Nakamura,[2] Haruo Matsuda,[2] Takeshi Yamazaki,[3] Ken-ichi Tanamoto[3] and Jun-ichi Sawada[4]

Correspondence
Yutaka Kikuchi
kikuchi@nihs.go.jp

[1,3,4]Division of Microbiology[1], Division of Food Additives[3] and Division of Biochemistry and Immunochemistry[4], National Institute of Health Sciences, 1-18-1 Kamiyoga, Setagaya-ku, Tokyo 158-8501, Japan

[2]Laboratory of Immunobiology, Graduate School of Biosphere Science, Hiroshima University, 1-4-4 Kagamiyama, Higashi-hiroshima, Hiroshima 739-8528, Japan

Human prion diseases, such as Creutzfeldt–Jakob disease (CJD), a lethal, neurodegenerative condition, occur in sporadic, genetic and transmitted forms. CJD is associated with the conversion of normal cellular prion protein (PrP^{C}) into a protease-resistant isoform (PrP^{res}). The mechanism of the conversion has not been studied in human cell cultures, due to the lack of a model system. In this study, such a system has been developed by culturing cell lines. Human glioblastoma cell line T98G had no coding-region mutations of the prion protein gene, which was of the 129 M/V genotype, and expressed endogenous PrP^{C} constitutively. T98G cells produced a form of proteinase K (PK)-resistant prion protein fragment following long-term culture and high passage number; its deglycosylated form was approximately 18 kDa. The PK-treated PrP^{res} was detected by immunoblotting with the mAb 6H4, which recognizes residues 144–152, and a polyclonal anti-C-terminal antibody, but not by the mAb 3F4, which recognizes residues 109–112, or the anti-N-terminal mAb HUC2-13. These results suggest that PrP^{C} was converted into a proteinase-resistant form of PrP^{res} in T98G cells.

Received 18 February 2004
Accepted 19 July 2004

INTRODUCTION

Fatal human prion diseases, including sporadic Creutzfeldt–Jakob disease (CJD), inherited prion diseases, iatrogenic CJD, kuru and variant CJD, are transmissible spongiform encephalopathies that are characterized by the formation and accumulation of an abnormal isoform of prion protein (PrP) in the brain (Prusiner, 2001). The PrP^{res} isoform is an insoluble aggregate that is resistant to proteinase K (PK) digestion. The conversion from cellular prion protein (PrP^{C}) into PrP^{res} could be a potential therapeutic target for prion diseases, but the mechanism of the conversion is unclear.

Several animal cell lines, including mouse neuroblastoma cells (Butler *et al.*, 1988; Race *et al.*, 1987), mouse hypothalamic neuronal cells (Nishida *et al.*, 2000; Schätzl *et al.*, 1997), mouse Schwann cells (Follet *et al.*, 2002) and rat pheochromocytoma cells (Rubenstein *et al.*, 1984), have been infected successfully with scrapie agents, and a human neuroblastoma cell line can also be infected with CJD agents (Ladogana *et al.*, 1995). These cells have been used to study the conversion mechanisms (Lehmann & Harris, 1997) and the subcellular localization (Naslavsky *et al.*, 1997; Vey *et al.*, 1996) of PrP^{res} and to evaluate therapeutic agents (Caughey & Raymond, 1993; Doh-Ura *et al.*, 2000). However, the efficiencies of infection and propagation of PrP^{res} are relatively low. The mouse cell line SMB was established from a scrapie-infected mouse brain (Clarke & Haig, 1970) and has been used to study the properties of PrP (Birkett *et al.*, 2001). Recently, stable cell lines were established from mouse peripheral neuroglial cells expressing ovine PrP and simian virus 40 T antigen. These cells were readily infectible by sheep PrP^{Sc}, a scrapie isoform of PrP (Archer *et al.*, 2004). However, there are currently no human cell lines that have been used to study the conversion mechanism from PrP^{C} into PrP^{res}.

PrP mRNA is expressed not only in neurons, but also in glia (Moser *et al.*, 1995) and PrP^{Sc} accumulates in the cytosol and cell-surface membrane of glial cells (van Keulen *et al.*, 1995). The role of glial cells in prion disease is not clear. Human glioblastoma T98G cells, like normal cells, become arrested in G_1 phase under stationary-phase conditions (Stein, 1979). In a previous study, we showed that T98G cells express PrP^{C} mRNA constitutively and produce a high level of endogenous PrP^{C} in G_1 phase (Kikuchi *et al.*, 2002). In the present study, we have investigated whether PrP^{C} is

converted into PrP^{res}, a marker for prion diseases, in cultured T98G cells under various conditions.

METHODS

Materials. A primer set for the human PrP coding sequence (CDS) (GenBank accession no. AL133396) [5′-CGAGGCAGAGCAGTCATT-3′, starting 18 nt before the ORF, and 5′-AGATGGTGAAAACGAGAAGAC-3′, ending 6 nt after the ORF (expected product size, 806 bp)] and an internal primer set (5′-GGCAGTGACTATGAGGACCGTTAC-3′ and 5′-GTAACGGTCCTCATAGTCACTGCC-3′, corresponding to nt 424–447 relative to the start site of the ORF) were synthesized chemically. Peptide *N*-glycosidase F (PNGase F) and *Bsa*AI were purchased from New England Biolabs and RPMI 1640 medium was purchased from Nissui Pharmaceutical. A BCA protein assay kit and SuperSignal West Femto Maximum Sensitivity substrate were from Pierce Biotechnology. Hybond-P PVDF membranes were purchased from Amersham Biosciences. Anti-human PrP mAb 3F4 was purchased from Signet Laboratories and 6H4 from Prionics AG. Fetal calf serum (FCS), horseradish peroxidase (HRP)-conjugated goat anti-mouse IgG, HRP-conjugated goat anti-rabbit IgG, HRP-conjugated rabbit anti-chicken IgG, aprotinin, leupeptin, PMSF, 4-methylumbelliferyl-β-D-galactoside (4-MUG) and mouse IgG were purchased from Sigma. PK was purchased from Merck and 4-(2-aminoethyl)-benzenesulfonyl fluoride hydrochloride (AEBSF) from Roche Diagnostics. SuperScript II reverse transcriptase and random primers were purchased from Invitrogen. β-Galactosidase-conjugated goat anti-mouse IgG was purchased from American Qualex, DNase I from Takara, KOD-Plus-DNA polymerase from Toyobo and 1,4-diazabicyclo[2.2.2]octane (DABCO) from Nacalai Tesque.

Preparation of antibodies. The preparation of chicken mAb HUC2-13 (IgG) against human PrP peptide residues 25–49 was reported previously (Matsuda *et al.*, 1999). The preparation of rabbit polyclonal antibody HPC2 (IgG) against human PrP peptide residues 214–230 was also reported previously (Kikuchi *et al.*, 2002).

Cell culture. Human glioblastoma cell line T98G (JCRB9041) at nominal passage level 433 was provided by the Japanese Cancer Research Resources Bank (Tokyo, Japan). Human astrocytoma U373MG cells were kindly provided by Dr T. Kasahara (Kyoritsu College of Pharmacy, Tokyo, Japan). Cell cultures stored in liquid nitrogen were thawed as passage 0 (P0) and cultured at 37 °C in monolayers on a T75 plastic tissue-culture flask in RPMI 1640 medium supplemented with 10% (v/v) heat-inactivated FCS, 60 μg kanamycin ml^{-1} and 10 mM HEPES/NaOH, pH 7·2. All cell lines were subcultivated routinely at a 1:5 or 1:10 split ratio once a week.

PCR direct sequencing and RFLP analysis. Extraction of total RNA from the cells and RT-PCR analysis were performed according to a published method (Kikuchi *et al.*, 2002) with slight modifications. Briefly, 5 μg total RNA was treated with DNase I for 15 min at room temperature. Random primers and SuperScript II reverse transcriptase were added to 20 μl (2·5 μg total RNA) and the mixture was incubated at 42 °C for 60 min to synthesize cDNA. Subsequently, 10 μl cDNA solution was subjected to PCR in a total volume of 50 μl, which included 0·2 mM dNTPs, 1 mM $MgSO_4$, 1 U KOD-Plus-DNA polymerase and 50 pmol sense and antisense primers. The amplification programme was as follows: denaturation at 94 °C for 20 s, annealing at 60 °C for 30 s and elongation at 68 °C for 60 s for 40 cycles. Final elongation was performed at 68 °C for 1 min. PCR was carried out in a GeneAmp PCR system 2400 (Applied Biosystems). PCR direct sequencing was performed with a CEQ 2000XL DNA Analysis system (Beckman Coulter) using the primer set for human PrP CDS and an internal primer. Codon 129 polymorphisms were detected by RFLP analysis; the PCR product (200 ng DNA) was digested with 5 U *Bsa*AI for 60 min at 37 °C; after incubation for 20 min at 80 °C, restriction fragments were separated by electrophoresis in 2% agarose gels and visualized following ethidium bromide staining.

Preparation of whole-cell lysates. All cell lines were plated at $5·0 \times 10^5$ cells per 9 cm dish (55 cm^2) in 10 ml medium on day 0 (D0). The medium was changed every 4 days. At the indicated times, cells were washed twice with ice-cold PBS and scraped into lysis buffer [$1·8 \times 10^4$ cells μl^{-1}; 10 mM Tris/HCl (pH 7·5), 150 mM NaCl, 1% sodium deoxycholate, 0·1% SDS, 1% NP-40, 10 mM NaF, 1 mM EDTA, 0·5 mM Na_3VO_3, 10 mM tetrasodium pyrophosphate] with protease inhibitor cocktail [0·06 trypsin inhibitor units (TIU) aprotinin ml^{-1}, 20 μM leupeptin and 1 mM PMSF]. After sonication, insoluble material was pelleted by centrifugation at 500 *g* for 15 min at 4 °C to yield whole-cell lysates. Protein concentration was determined by the BCA protein assay.

Subcellular fractionation. At the indicated times, cells were washed twice with ice-cold PBS and scraped into PBS/2·5 mM EDTA with the protease inhibitor cocktail. After sonication, insoluble material was pelleted by centrifugation at 500 *g* for 15 min at 4 °C to yield homogenates. The postnuclear fraction was centrifuged at 100 000 *g* for 60 min at 4 °C to obtain a cytosolic fraction and a membrane fraction. The membrane fraction was dissolved in PBS/2·5 mM EDTA with the protease inhibitor cocktail. Protein concentration was determined by the BCA protein assay.

Detergent solubility test. A detergent solubility test was carried out according to a described method (Capellari *et al.*, 2000) with slight modifications. Cells were washed twice with ice-cold PBS and scraped into PBS/2·5 mM EDTA with the protease inhibitor cocktail. After sonication, insoluble material was pelleted by centrifugation at 500 *g* for 15 min at 4 °C to yield homogenates. The postnuclear fraction was dissolved in 9 vols 0·5% NP-40/0·5% deoxycholate/PBS with the protease inhibitor cocktail and centrifuged at 100 000 *g* for 60 min at 4 °C to obtain a detergent-insoluble pellet fraction and a soluble supernatant fraction. The supernatant fraction was precipitated with 4 vols methanol for 16 h at −20 °C. Both fractions were resuspended in the same volume of lysis buffer.

Protease-resistant PrP assay. To generate material for the protease-resistant PrP assay, aliquots of the sample (50 μg protein) were precipitated with 4 vols methanol for 16 h at −20 °C to remove the protease inhibitor cocktail (Capellari *et al.*, 2000), centrifuged at 14 000 *g* for 15 min at 4 °C and the pellet was dissolved in 50 mM Tris/HCl (pH 7·2). Samples were treated with PK (at 10 μg ml^{-1} unless stated otherwise) at 37 °C for 30 min, according to a described method (Caughey *et al.*, 1999). After incubation, digestion was stopped by the addition of AEBSF to 4 mM. Samples were prepared with the protease inhibitor cocktail at a concentration that did not inhibit the activity of PK (Fig. 1a, lane 1).

Enzymic deglycosylation. For the removal of Asn-linked oligosaccharides, aliquots of whole-cell lysates were treated with PNGase F as follows (Kikuchi *et al.*, 2002): lysates (50 μg protein) were denatured by boiling for 10 min in 0·5% SDS, 1% 2-mercaptoethanol. After addition of NP-40 to 1%, the lysates were incubated at 37 °C for 2 h with 0·77 IUB mU PNGase F in 50 mM phosphate buffer (pH 7·5).

Immunoblotting. Usually, 50 μg total protein (prepared from approximately $1·7 \times 10^5$ cells) was subjected to SDS gel electrophoresis. Briefly, aliquots of the samples were mixed with 2× electrophoresis sample buffer. After boiling for 10 min, the samples

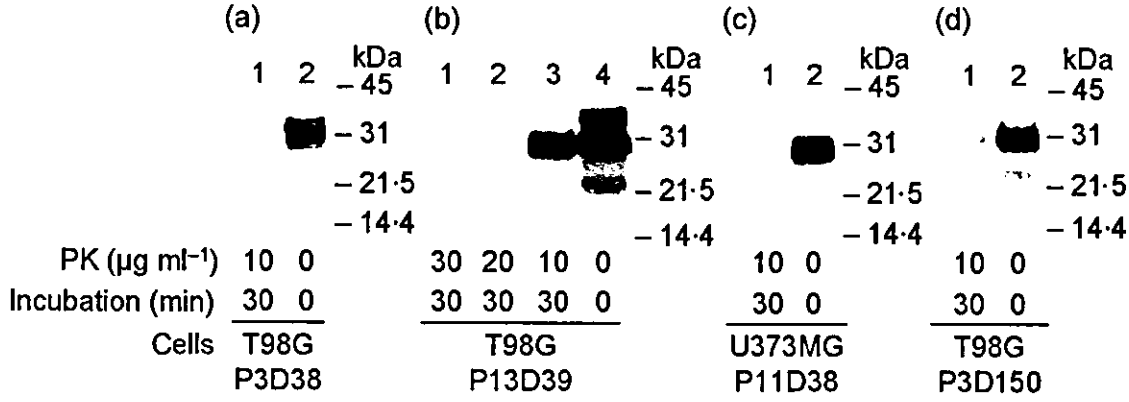

Fig. 1. Formation of a protease-resistant form of PrP in T98G cells is increased in a long-term incubation after repeated passages. T98G cells and U373MG cells were incubated under the following conditions with 10% FCS/RPMI 1640 and whole-cell, methanol-precipitated lysates (50 μg protein) were treated with PK (10 μg ml^{-1} unless stated otherwise) at for 30 min at 37 °C. (a) T98G cells were incubated for 38 days after 3 passages (P3D38); lysates were treated with PK (lane 1) or left undigested (lane 2). (b) T98G cells were incubated for 39 days after 13 passages (P13D39); lysates were treated with 10, 20 or 30 μg PK ml^{-1} (lanes 1–3) or left undigested (lane 4). (c) U373MG cells were incubated for 38 days after 11 passages (P11D38); lysates were treated with PK (lane 1) or left undigested (lane 2). (d) T98G cells were incubated for 150 days after 3 passages; lysates were treated with PK (lane 1) or left undigested (lane 2). PK-treated lysates were subjected to immunoblot with the 6H4 antibody as described in Methods.

were electrophoresed on 12·5% acrylamide gel and the proteins were transferred onto PVDF membranes. The membranes were blocked with 0·5% casein in PBS (casein/PBS) and incubated with anti-prion antibodies in casein/PBS. Immunoreactive bands were visualized with HRP-conjugated anti-IgG and SuperSignal West Femto Maximum Sensitivity substrate, according to the manufacturer's instructions (Pierce Biotechnology).

Indirect immunofluorescence staining. T98G cell monolayers grown on a 15 mm glass coverslip (Matsunami) in a 9 cm dish (55 cm^2) were maintained in 10 ml medium. At the indicated times, cells were washed twice with ice-cold PBS and then fixed with 3·7% formaldehyde in PBS for 30 min at 4 °C. The fixed cells were washed twice with PBS and then treated with 0·2% Triton X-100 in PBS for 15 min at room temperature. The cells were blocked with 10% normal goat serum in PBS (NGS/PBS) for 60 min and incubated with antibody (100 ng ml^{-1}) for 16 h at 4 °C. After extensive washing with 0·05% Tween 20/PBS, cells were treated with Alexa 594 goat anti-mouse IgG (H+L) conjugate (5 μg ml^{-1}) (Molecular Probes) in NGS/PBS for 1 h at 4 °C, washed with 0·05% Tween 20/PBS and mounted with 2·5% DABCO/90% glycerin/PBS. The stained cells were observed and photographed with the aid of a fluorescence microscope (Olympus).

Competitive ELISA. ELISA was carried out according to a method described previously (Kikuchi *et al.*, 1991). For a dilution buffer, casein/PBS was used throughout the present study. Briefly, the wells were coated with 100 ng recombinant bovine PrP (rBoPrP) (Takekida *et al.*, 2002) in PBS and left at 4 °C overnight. Appropriately diluted standard rBoPrP solutions or samples were added to the antigen-coated wells and incubated at room temperature for 60 min, in a total volume of 50 μl, with 6H4 antibody (460 pg). The wells were washed, incubated with β-galactosidase-conjugated goat anti-mouse IgG for 60 min, washed again and then incubated with 4-MUG as a substrate at 37 °C for 60 min. Enzyme activity was determined by fluorescence intensity measurements.

RESULTS

Production of protease-resistant isoform of PrP in T98G cells

We analysed whole-cell lysates of long-term cultured T98G cells by immunoblotting with anti-PrP antibodies. When we cultured the cells for 38 days after 3 passages [passage 3, day 38 (P3D38)], the lysates revealed two bands (35 and 31 kDa) that reacted with mouse anti-human PrP mAb 6H4 (Fig. 1a, lane 2) and were destroyed completely after digestion with PK (Fig. 1a, lane 1). When lysates from cells that were cultured for 39 days after 13 passages [passage 13, day 39 (P13D39)] were digested with PK (10, 20 or 30 μg ml^{-1}), the 35 kDa band, but not the 31 kDa band, was diminished (Fig. 1b), indicating the presence of PrP^{res}. We then attempted to detect PrP^{res} formation in long-term cultures of another human glial cell line, U373MG, an astrocytoma line that expresses consistently high levels of PrP^{C} mRNA (Satoh *et al.*, 1998). The lysates from P11D38 U373MG cells exhibited the 31 kDa band that reacted with the 6H4 antibody and disappeared after digestion with PK (Fig. 1c). Lysates from P3D150 T98G cells showed a faint 31 kDa band after PK treatment (Fig. 1d). In contrast, P13D39 T98G cells had produced highly PK-resistant PrP. These data indicated that PrP^{res} propagation in T98G cells required not only long-term culture, but also a high passage number.

Examination of phenotypic variants of PrP^{res}

We first asked whether an inherited or a sporadic CJD-like form of PrP^{res} was propagated in T98G cells. Inherited prion

diseases are determined by mutations in the 762 bp CDS of the prion protein gene (*PRNP*) (Kovács *et al.*, 2002). We performed PCR direct sequencing of the *PRNP* mRNA that was expressed in short- and long-term cultured T98G cells and found no mutations other than the presence of both adenine and guanine at the first position of codon 129 (the basis of the common M129V polymorphism) (data not shown). When digested by *Bsa*AI, the 806 bp PCR product from the M129V haplotype (Fig. 2a, lane 1) yielded products of 402 and 404 bp and also undigested wild-type product (Fig. 2a, lane 2), which we confirmed by RFLP analysis. These results indicated that T98G cells were heterozygotes, having both methionine and valine at codon 129 of *PRNP* with no coding-region mutation.

Next, to estimate the size of the deglycosylated PrP^{res}, we treated the lysates from P40D40 T98G cells with PK and/or PNGase F. PNGase F yields a full-length (25 kDa) and an N-terminally truncated (18 kDa) form of PrP^{C} (Kikuchi *et al.*, 2002). As shown in Fig. 2b, PNGase F treatment reduced the glycosylated 35 and 31 kDa bands (lane 4) to 25 and 18 kDa (lane 3), representing the deglycosylated full-length and N-terminally truncated forms. An additional PNGase F treatment changed fully glycosylated (31 kDa) and partially glycosylated (23 kDa) forms of PrP^{res}, detectable after digestion with PK (lane 2), to an unglycosylated form of 18 kDa (lane 1). These results established that the size of the deglycosylated PK-resistant fragment in T98G cells was approximately 18 kDa.

Confirming heterogeneity of PrP^{res} by immunoblotting with sets of anti-PrP antibodies

To further investigate the heterogeneity of PrP^{res} from long-term cultured T98G cells, we determined the antigenicity of PrP^{res}. By immunoblotting with sets of antibodies to PrP (Kikuchi *et al.*, 2002), we detected a full-length PrP (35 kDa) in lysates from P40D40 T98G cells that reacted with the anti-N terminus PrP antibody HUC2-13 (Fig. 3a, lane 2), as well as with the 6H4 antibody (Fig. 3c, lane 2). Following PK treatment of the lysates, the 31 kDa band was still detected by 6H4 antibody (Fig. 3c, lane 1), but not by HUC2-13 antibody (Fig. 3a, lane 1), indicating that PK treatment had cleaved the N terminus of PrP^{res}. The 31 kDa band was also detected by the anti-C terminus PrP antibody HPC2 (Fig. 3d, lane 1). HPC2 antibody, which reacts strongly with the deglycosylated form of PrP^{C}, but weakly with the glycosylated form (Kikuchi *et al.*, 2002), also recognized the N-terminally truncated form of PrP^{res}. Surprisingly, the 3F4 antibody, which recognizes residues 109–112, failed to detect the N-terminally truncated form of PrP^{res} (Fig. 3b), such as is seen with the HUC2-13 antibody (Fig. 3a). These experiments showed that the N-terminally truncated form of PrP^{res} in T98G cells lacks the epitope that is recognized by the 3F4 antibody.

Subcellular localization and detergent solubility of PrP^{res} in T98G cells

To determine the subcellular localization of PrP^{res}, we studied the distribution of PrP in P40D40 T98G cells

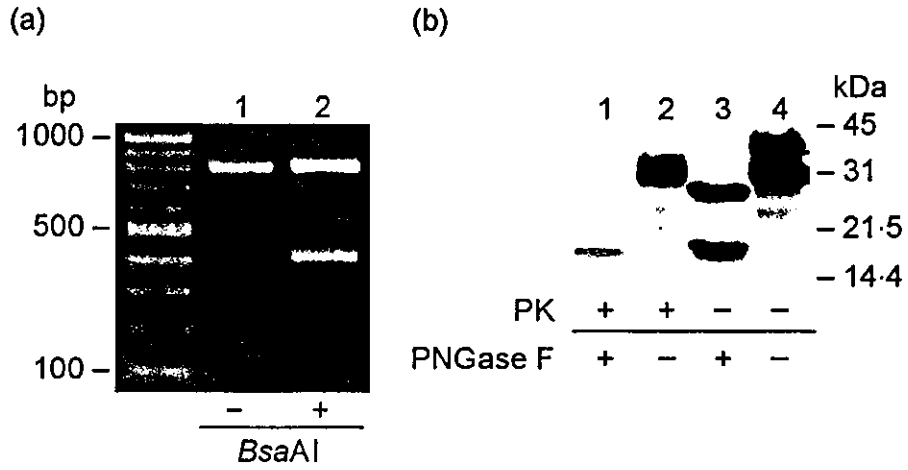

Fig. 2. Molecular analysis of PrP^{res} in T98G cells. (a) Detection of polymorphism at codon 129 on PrP mRNA in T98G cells. T98G cells were incubated with 10% FCS/RPMI 1640 for 5 days after 43 passages (P43D5) and total RNA was prepared, reverse-transcribed and PCR-amplified as described in Methods and digested with *Bsa*AI (lane 2) or left undigested (lane 1). A DNA size marker (100 bp ladder) is shown on the left. (b) Analysis of deglycosylated forms of PrP in T98G cells. T98G cells were incubated with 10% FCS/RPMI 1640 for 40 days after 40 passages (P40D40); whole-cell, methanol-precipitated lysates were treated with PK (lanes 1 and 2) or left undigested (lanes 3 and 4). All lysates were incubated with (lanes 1 and 3) or without (lanes 2 and 4) PNGase F for 120 min. PK-treated lysates were subjected to immunoblot with the 6H4 antibody as described in Methods.